**University of Alberta**

**Library Release Form**

**Name of Author**: Xinwei Deng

**Title of Thesis**: Performance Analysis of Orthogonal Space-Time Block-Coded MIMO Systems with Antenna Selection

**Degree**: Master of Science

**Year this Degree Granted**: 2007

_____

Xinwei Deng

**Date**: _____

**University of Alberta**


PERFORMANCE ANALYSIS OF ORTHOGONAL SPACE-TIME BLOCK-CODED MIMO
SYSTEMS WITH ANTENNA SELECTION


by


**Xinwei Deng**


A thesis submitted to the Faculty of Graduate Studies and Research in partial fulfillment
of the requirements for the degree of **Master of Science**.


Department of Electrical and Computer Engineering


Edmonton, Alberta

Fall 2007

**University of Alberta**

**Faculty of Graduate Studies and Research**

The undersigned certify that they have read, and recommend to the Faculty of Graduate Studies and Research for acceptance, a thesis entitled **Performance Analysis of Orthogonal Space-Time Block-Coded MIMO Systems with Antenna Selection** submitted by Xinwei Deng in partial fulfillment of the requirements for the degree of **Master of Science**.

———————————————————

Chintha Tellambura (Supervisor)

———————————————————

Externalperson (External)

———————————————————

Sergiy Vorobyov

———————————————————

Janelle Harms

**Date**: ————————————

# Abstract

Antenna selection reduces the system cost and complexity by reducing the number of radio frequency (RF) chains while still retaining full diversity. Despite extensive research on receive antenna selection (RAS), the analysis of transmit antenna selection (TAS) and transmit and receive antenna selection (T-RAS) encounters problems due to statistical difficulties. In this thesis, performance analysis using a simple measurement known as amount of fading (AF) is provided. Approximations and bounds for the AF as well as methods to derive the exact AF calculations for TAS on Rayleigh fading channels are derived. A simple approximate formula for the relationship between the AF and the coding gain in a TAS system is achieved. Furthermore, the average bit error rate (BER), average symbol error rata (SER), outage probability and ergodic capacity are derived by utilizing the characteristic function (CF) of the joint output signal-to-noise ratios (SNR) in generalized T-RAS systems. This approach can be used for both independent and arbitrarily correlated Rayleigh, Nakagami-$m$ and Rician fading channels. The effects of the antenna array configuration and the operating environment (fading, angular spread, mean angle-of-arrival (AOA), mean angle-of-departure (AOD)) on the average BER performance are illustrated. The simulation results are provided to validate the numerical calculations.

# Acknowledgements

I would like to take the opportunity to thank all the people who have supported me throughout my master study.

First, I would like to thank Dr. Tellambura, my supervisor, for his great support for the past two years. I cherish all the help he had given me. He has led me into this promising field and offered much of his insight as well as kindness to a beginner as me. I will bear in mind all the things I have learnt here including the attitudes towards different things. They are also a priceless treasure for my future endeavor.

I like to thank Dr. Sergiy Vorobyov and Dr. Janelle Harms for their precious time and effort to be my committees.

A great gratitude goes to Wei Zhang, who was my co-researcher in most of the works and offered me much help. I would also like to thank all iCORE Wireless Communications Laboratory members, who helped me in one way or another with their warmheart and sincerity.

I also wish to thank the Alberta Informatics Circle of Research Excellence (iCORE) for their financial support.

From the deepest of my heart, I would give special thanks to my family who are always there supporting me, reminding me and encouraging me. I am really grateful for their caring and understanding.

# Contents

# List of Figures

# Acronyms

| Acronyms | Definition |
| --- | --- |
| A/D | analog to digital |
| AF | amount of fading |
| AOA | angle-of-arrival |
| AOD | angle-of-departure |
| AWGN | additive white Gaussian noise |
| BER | bit error rate |
| BFSK | binary frequency shift keying |
| BPSK | binary phase shift keying |
| CF | characteristic function |
| CDF | cumulative distribution function |
| D/A | digital-to-analog |
| EGC | equal gain combiner |
| GSC | Generalized selection combining |
| i.i.d. | independent identically distributed |
| LNA | low noise amplifier |
| LOS | line-of-sight |
| MGF | moment generating function |
| M-PSK | $M$-ary phase shift keying |
| M-QAM | $M$-ary square amplitude modulation |
| MRC | maximum ratio combining |

| | |
|---|---|
| MIMO | multiple input multiple output |
| ML | maximum-likelihood |
| OSTBC | orthogonal space-time block codes |
| PDF | probability density function |
| PSK | phase shift keying |
| QPSK | quadrature phase shift keying |
| RAS | receive antenna selection |
| RF | radio frequency |
| SC | selection combining |
| SER | symbol error rate |
| SISO | single input single output |
| SNR | signal-to-noise ratio |
| TAS | transmit antenna selection |
| ULA | uniform linear arrays |
| T-RAS | transmit and receive antenna selection |
| WCDMA | wideband code division multiple access |
| ZMCSCG | zero mean circularly symmetric complex Gaussian |

# List of Symbols

| Notations | Definition |
|---|---|
| $\mathscr{E}(x)$ | expectation of random variable $x$ |
| $\text{var}(x)$ | statistical variance of random variable $x$ |
| $E_s$ | energy per symbol |
| $f(x)$ | PDF of random variable $x$ |
| $f(x_1, \cdots, x_n)$ | joint PDF of random variables $x_1, \cdots, x_n$ |
| $F(x)$ | CDF of random variable $x$ |
| $M(x)$ | MGF of random variable $x$ |
| $\min(a, b)$ | minimum of a and b |
| $(\mathbf{A})^{1/2}$ | the square root of matrix $\mathbf{A}$ |
| $r(\mathbf{A})$ | rank of $\mathbf{A}$ |
| $(\cdot)^*$ | complex conjugate operator |
| $(\cdot)^{-1}$ | matrix inverse operator |
| $(\cdot)^T$ | transpose operator |
| $(\cdot)^H$ | conjugate transpose operator |
| $\mathbf{A}(m, n)$ | the $(m, n)$-th entry of $\mathbf{A}$ |
| $\det(\mathbf{A})$ | determinant of $\mathbf{A}$ |
| $\text{vec}(\mathbf{A})$ | vectorization of $\mathbf{A}$ |
| $\|\mathbf{A}\|_F^2$ | Frobenius norm of $\mathbf{A}$ |
| $\mathbf{A} \otimes \mathbf{B}$ | Kronecker product of the matrices $\mathbf{A}$ and $\mathbf{B}$ |
| $\mathscr{CN}(\mu, \sigma^2)$ | a circularly complex Gaussian variable with mean $\mu$ and variance $\sigma^2$ |

| | |
|---|---|
| $\mathcal{N}(\mu,\sigma^2)$ | a Gaussian variable with mean $\mu$ and variance $\sigma^2$ |
| $\Gamma(\cdot)$ | the Gamma function |
| $I_m(\cdot)$ | the $m$-th order modified Bessel function |
| $\mathcal{Q}(\cdot,\cdot)$ | the first order Marcum Q-function |
| $Q(\cdot)$ | the Gaussian Q-function |
| $\gamma(\cdot,\cdot)$ | the complementary incomplete gamma function |
| $\mathscr{C}^{m\times n}$ | a $m \times n$-dimensional complex matrix space |

# Chapter 1

# Introduction

## 1.1  Motivation

The wireless communication industry has been experiencing phenomenal growth rates over the past several years.  In many applications, wireless can eliminate the high costs of installing and maintaining traditional wired systems.  Wireless services are accessible even in the most rural community.  However, the largest obstacle facing designers of wireless communication systems is the random nature of the wireless propagation channel.  The wireless channel is non-stationary and noisy due to fading and interference.  Recent advances have demonstrated that multiple-input-multiple-output (MIMO) wireless systems can significantly improve the system performance.  MIMO technology has thus got the potential to provide the next major leap forward for wireless communications [1].

However, MIMO systems have increased complexity and cost compared to traditional single-input single-output (SISO) systems.  While additional antenna elements (patch or dipole antennas) are inexpensive, the radio frequency (RF) elements are expensive. MIMO systems with $N_t$ transmit and $N_r$ receive antennas require $N_t$ ($N_r$) complete RF chains at the transmitter and the receiver, respectively, including low-noise amplifiers, downconverters, and analog-to-digital converters.

Due to this reason, there is an increasing interest in antenna selection schemes, where

the 'best' antenna subset of available antennas are chosen (either at one or both link ends), downconverted, and processed. This selection reduces the number of required RF chains, and thus, leads to significant savings in cost and complexity. The savings come at the price of a (usually small) performance loss compared to the full-complexity system [2].

Several types of antenna selection are possible: Transmit Antenna Selection (TAS), Receive Antenna Selection (RAS), and Transmit and Receive Antenna Selection (T-RAS). Antenna selection attempts to choose the sub-channels that have the 'best' performance in terms of bit error rate (BER) or capacity. When orthogonal space-time block codes (OSTBCs) are used for transmission, the system is guaranteed to have full diversity but with a less system cost [2].

## 1.2  Contributions

In this thesis, we analyze MIMO antenna selection with OSTBCs under both independent and correlated fading channels.

- The amount of fading (AF) is derived for general MIMO systems with independent and identically distributed (i.i.d.) Rayleigh fading channels. Methods of deriving the exact AF for MIMO TAS systems are provided. Upper bounds and lower bounds are derived. A simple approximate AF formula is derived.

- Upper bounds and lower bounds on the AF are derived for fading channels with correlation. Simple approximation formulas are derived for the constant correlation model at the receiver side.

- A simple relationship between the AF and the symbol error rate (SER) is given under i.i.d. fading channels and TAS. Correspondingly, a simple relationship between the AF and coding gain is provided.

- By utilizing characteristic function (CF), the average BER, SER, outage probability, ergodic capacity are derived for correlated channels in T-RAS MIMO systems.

Results are extended to Rayleigh, Nakagami-*m* and Rician fading channels.

- The effects of the antenna array configuration and the operating environment (fading, angular spread, mean angle-of-arrival (AOA), mean angle-of-departure (AOD)) on the average BER performance are illustrated.

## 1.3    Thesis Outline

The thesis is organized as follows:

- Chapter 2 provides an overview on general MIMO channels and antenna selection schemes.

- Chapter 3 deals with AF analysis under both independent and correlated channels in MIMO TAS systems. A simple relationship between AF, SER and coding gain is also provided.

- In Chapter 4, a general framework for analyzing antenna selection is introduced. It allows the derivation of SER, BER, outage probability as well as ergodic capacity. The effects of antenna array configuration and the operating environment are also illustrated. Numerical results are given to validate derived results.

- Conclusions and future work are given in Chapter 5.

# Chapter 2

# MIMO Systems with Antenna Selection

In this chapter, MIMO systems with antenna selection are briefly overviewed. Statistical assumptions and correlation models are presented in Section 2.2. In Section 2.3, common performance measures are discussed. Different antenna selection schemes are introduced in Section 2.4, along with a general system model under OSTBC.

## 2.1   Introduction

MIMO wireless systems, also known as multiple-antenna systems, have multiple antenna elements at both the transmitter and receiver [3]. They were first analyzed in the 1980s and 1990s [4–6]. The interest in MIMO systems has exploded ever since. They are now being used for the third-generation cellular systems and for future high-performance modes of the highly successful IEEE 802.11 standard for wireless local area networks [7].

Obtaining the full benefits of multiple transmit antennas may however require the use of space-time signaling schemes such as OSTBCs, a class of easily decodable space-time codes that achieves the full diversity order [8]. The family of OSTBCs simplifies the maximum likelihood (ML) decoding. However, a major limiting factor in the deployment of MIMO systems is the cost of multiple RF chains (each RF chain requires an amplifier, mixer, analog-to-digital converters and so on) at both ends of a wireless link. A powerful solution is to select a subset of the available antennas while keeping the advantages of

using all antennas [1]. This results in a limited number of RF chains being dynamically multiplexed between several transmit/receive antennas. In literature, RAS is a traditionally well-researched topic [1,9] and the study of TAS is more recent [10–12].

## 2.2 System Models

### 2.2.1 Statistical Models of MIMO Fading Channels

Consider a wireless communication system with $N_t$ transmit and $N_r$ receive antennas. The quasi-static flat fading MIMO channel can be represented in a matrix form as [13]:

$$\mathbf{H} = \begin{bmatrix} h_{1,1} & h_{1,2} & \cdots & h_{1,N_t} \\ h_{2,1} & h_{2,2} & \cdots & h_{2,N_t} \\ \dotfill \\ h_{N_r,1} & h_{N_r,2} & \cdots & h_{N_r,N_t} \end{bmatrix} \tag{2.1}$$

where $h_{i,j}$ ($1 \leq i \leq N_r$, $1 \leq j \leq N_t$) is the channel gain between the $j$-th transmit antenna and the $i$-th receive antenna. Note that $h_{i,j}$ is the composite channel impulse response inclusive of the pulse-shaping filter at the $j$-th transmitter, the propagation channel and the $i$-th receiver matched-filter. The special case in which the elements $h_{i,j}$ are i.i.d. zero mean circularly symmetric complex Gaussian (ZMCSCG) with unit variance is called the spatially white channel $\mathbf{H}_w$ [13].

The squared Frobenius norm of $\mathbf{H}$, i.e., $\|\mathbf{H}\|_F^2$, is defined as

$$\|\mathbf{H}\|_F^2 = Tr(\mathbf{H}\mathbf{H}^H) = \sum_{i=1}^{N_r} \sum_{j=1}^{N_t} |h_{i,j}|^2. \tag{2.2}$$

Due to the randomness of $\mathbf{H}$, $\|\mathbf{H}\|_F^2$ is also a random variable. The statistics of $\|\mathbf{H}\|_F^2$ determines the diversity performance. When $\mathbf{H} = \mathbf{H}_w$, the probability density function (PDF) of $\|\mathbf{H}\|_F^2$ is given by [14]

$$f(x) = \frac{x^{N_t N_r - 1}}{(N_t N_r - 1)!} e^{-x}. \tag{2.3}$$

5

Therefore, $\|\mathbf{H}\|_F^2$ is a chi-squared random variable with $2N_tN_r$ degrees of freedom [15].

The channel gain $h_{i,j}$ for all $i, j$ is commonly described using several different statistical models. Usually, to analyze the performance of MIMO systems, the cumulative distribution function (CDF), PDF and the moment generating function (MGF) of the fading amplitudes are often required.

## Rayleigh Distribution

In urban and suburban areas, when fading is caused by the superposition of a large number of independent scattered components, the envelope of the received signal can be modeled as a Rayleigh distribution [13]. Let $X = \sqrt{X_1^2 + X_2^2}$ where $X_1$ and $X_2$ are independent zero-mean Gaussian random variables with common variance $\sigma^2$, i.e. $X_1, X_2 \sim N(0, \sigma^2)$. Thus, $X$ is Rayleigh distributed with the PDF given by

$$f_X(x) = \frac{x}{\sigma^2} e^{-\frac{x^2}{2\sigma^2}}, \quad x \geq 0. \tag{2.4}$$

The squared-envelope is central chi-square distributed with two degrees of freedom, i.e. $X^2 \sim \chi_2(0, \sigma^2)$ or exponentially distributed, whose CDF, PDF and MGF are given respectively by [14]

$$F_{X^2}(y) = 1 - \exp\left(-\frac{y}{2\sigma^2}\right), \quad y \geq 0 \tag{2.5}$$

$$f_{X^2}(y) = \frac{1}{2\sigma^2} \exp\left(-\frac{y}{2\sigma^2}\right), \quad y \geq 0 \tag{2.6}$$

$$M_{X^2}(s) = \frac{1}{1 + 2\sigma^2 s}, \quad s > -\frac{1}{2\sigma^2}. \tag{2.7}$$

## Rician Distribution

In rural regions, on the other hand, the received signal contains a direct line-of-sight (LOS) component; thus the envelope of received signal follows the Rician distribution [13]. Let $X = \sqrt{X_1^2 + X_2^2}$ where $X_1$ and $X_2$ are independent Gaussian random variables with non-zero means $m_1$, $m_2$ and common variance $\mathscr{E}[(X_1 - m_1)^2] = \mathscr{E}[(X_2 - m_2)^2)] = \sigma^2$ and $\mathscr{E}(x)$ represents the expectation of the random variable $x$, i.e. $X_1 \sim N(m_1, \sigma^2)$ and $X_2 \sim N(m_2, \sigma^2)$.

Then $X$ is Rician distributed with the Rician factor $K = \frac{m_1^2 + m_2^2}{2\sigma^2}$, the average power $\Omega = \mathscr{E}(X^2) = m_1^2 + m_2^2 + 2\sigma^2$, i.e. $X \sim \mathscr{R}\left(\frac{m_1^2 + m_2^2}{2\sigma^2}, m_1^2 + m_2^2 + 2\sigma^2\right)$, and its PDF is given by

$$f_X(x) = \frac{x}{\sigma^2} \exp\left[-\frac{x^2 + m_1^2 + m_2^2}{2\sigma^2}\right] I_0\left(\frac{x\sqrt{m_1^2 + m_2^2}}{\sigma^2}\right), \quad x \geq 0 \tag{2.8}$$

where $I_0(x)$ is the zero-th order modified Bessel function of the first kind, as given by

$$I_0(x) = \frac{1}{\pi} \int_0^\pi e^{x\cos\theta}\, d\theta. \tag{2.9}$$

The squared-envelope of a Rician random variable is non-central chi-square distributed with two degrees of freedom, i.e. $X^2 \sim \chi_2(\sqrt{\frac{K\Omega}{K+1}}, \sigma^2)$, whose CDF, PDF, MGF are given respectively by [14]

$$F_{X^2}(y) = 1 - \mathscr{Q}\left(\sqrt{2K}, \sqrt{\frac{2(K+1)y}{\Omega}}\right), \quad y \geq 0 \tag{2.10}$$

$$f_{X^2}(y) = \frac{K+1}{\Omega} \exp\left[-K - \frac{(K+1)y}{\Omega}\right] I_0\left(2\sqrt{\frac{K(K+1)y}{\Omega}}\right), \quad y \geq 0 \tag{2.11}$$

$$M_{X^2}(s) = \frac{1+K}{1+K+s\Omega} \exp\left(-\frac{sK\Omega}{1+K+s\Omega}\right), \quad s > -\frac{1+K}{\Omega} \tag{2.12}$$

where $\mathscr{Q}(a,b)$ is the first order Marcum Q-function. The $m$-th order Marcum Q-function is given by

$$\mathscr{Q}_m(a,b) = \int_b^\infty x\left(\frac{x}{a}\right)^{m-1} \exp\left[-\frac{x^2 + a^2}{2}\right] I_{m-1}(ax)\, dx \tag{2.13}$$

where $I_m(x)$ is the $m$-th order modified Bessel function of the first kind. As expected, in the absence of a direct path ($K = 0$), the Rician PDF reduces to a Rayleigh PDF, confirming that the Rayleigh distribution is a special case of the Rician distribution [16, Apprendix B].

## Nakagami-$m$ Distribution

The Nakagami-$m$ distribution is a versatile statistical distribution which can accurately model a variety of fading environments. It has greater flexibility in matching some empirical data than the Rayleigh, Rician distributions. It includes the Rayleigh distribution as

a special case and can closely approximate the Rician distribution [17]. The PDF for this distribution is given by Nakagami [18]:

$$f_X(r) = \frac{2}{\Gamma(m)}(\frac{m}{\Omega})^m r^{2m-1} e^{-mr^2/\Omega} \tag{2.14}$$

where the average envelope power $\Omega$ is defined as

$$\Omega = \mathscr{E}(X^2) \tag{2.15}$$

$\Gamma(m)$ is the Gamma function which is defined by $\Gamma(x) = \int_0^\infty t^{x-1} e^{-t}$ and the parameter $m$, known as the fading figure, is defined as the ratio of moments

$$m = \frac{\Omega^2}{\mathscr{E}[(X^2 - \Omega)^2]}, \quad m \geq 1/2. \tag{2.16}$$

When $m = 1$ Eq. (2.14) reduces to the Rayleigh distribution. The squared-envelope of a Nakagami-$m$ random variable is Gamma distributed with CDF, PDF, and MGF given as [14]

$$F_{X^2}(y) = 1 - \frac{1}{\gamma(m)}\gamma(m, \frac{my}{\Omega}), \quad y \geq 0 \tag{2.17}$$

$$f_{X^2}(y) = \frac{1}{\gamma(m)}(\frac{m}{\Omega})^m y^{m-1} \exp(-\frac{my}{\Omega}), \quad y \geq 0 \tag{2.18}$$

$$M_{X^2}(s) = (\frac{m}{m+s\Omega})^m, \quad s > -\frac{m}{\Omega} \tag{2.19}$$

where $\gamma(a,x)$ is the complementary incomplete gamma function as defined by

$$\gamma(n,x) = \int_x^\infty t^{n-1} e^{-t} dt, \quad n \geq 0. \tag{2.20}$$

## 2.2.2 Spatial Fading Correlation

In $\mathbf{H_w}$ no correlation between different entries of the channel matrix is assumed. In practice, $\mathbf{H}$ can deviate significantly from $\mathbf{H}_w$ due to a variety of reasons. For example, inadequate antenna spacing and scattering lead to spatial correlation [13]. Thus, the entries of the channel matrix are no longer i.i.d.. Therefore, analysis of correlated fading channels has pratical significance.

8

The $N_t N_r \times N_t N_r$ correlation matrix $\mathbf{R}$ is defined as

$$\mathbf{R} = \mathscr{E}\{\mathrm{vec}(\mathbf{H})\,\mathrm{vec}(\mathbf{H})^H\} \tag{2.21}$$

where $\mathrm{vec}(\mathbf{A})$ stacks $\mathbf{A}$ into a vector column and superscript $(.)^H$ is the Hermitian operator. The correlated channels can be expressed in terms of the spatially-white channel:

$$\mathrm{vec}(\mathbf{H}) = \mathbf{R}^{1/2}\,\mathrm{vec}(\mathbf{H}_w) \tag{2.22}$$

where $\mathbf{H}_w$ is the spatially white $N_r \times N_t$ MIMO channel described earlier and $(\mathbf{A})^{1/2}$ denotes the square root of matrix $\mathbf{A}$.

Note that $\mathbf{R}$ is a positive semi-definite Hermitian matrix. If $\mathbf{R} = \mathbf{I}_{N_r N_t}$, then $\mathbf{H} = \mathbf{H}_w$. When the correlation properties at the transmitter are independent of those at the receiver, a simpler model is given by [13]

$$\mathbf{H} = \mathbf{R}_r^{1/2}\mathbf{H}_w\mathbf{R}_t^{1/2} \tag{2.23}$$

where $\mathbf{R}_r$ is the $N_r \times N_r$ receive correlation matrix, $\mathbf{R}_t$ is the $N_t \times N_t$ transmit correlation matrix. Note that $\mathbf{R}_r$ and $\mathbf{R}_t$ are positive semi-definite Hermitian matrices. Since the total correlation matrix is decomposed into transmit and receive parts, this model has fewer degrees of freedom than the model in Eq. (2.22). In this model, the receive antenna correlation $\mathbf{R}_r$ is equal to the correlation of the $N_r \times 1$ receive vector when excited by any transmit antenna, and is therefore the same for all transmit antennas. This condition holds when the angle spectra of the scatterers at the receive array for signals arriving from any transmit antennas are identical and happens if all the transmit antennas are closely located and have identical radiation patterns [13]. The conditions can also carry over to the case of transmit antenna correlation $\mathbf{R}_t$.

The three matrices $\mathbf{R}$, $\mathbf{R}_r$ and $\mathbf{R}_t$ are related as

$$\mathbf{R} = \mathbf{R}_t^T \otimes \mathbf{R}_r \tag{2.24}$$

where superscript $(.)^T$ is the transpose operator and $\otimes$ is the Kronecker product. Thus, the total channel correlation can be expressed as the Kronecker product of the transmitter and the receiver correlation matrices.

9

In the presence of receive or transmit correlation, the rank of $\mathbf{H}$ is reduced from full rank to $\min(r(\mathbf{R}_r), r(\mathbf{R}_t))$, where $r(\mathbf{A})$ is the rank of $\mathbf{A}$.

For Rayleigh fading, the MGF of the Frobenius norm of the channel denoted by $M_{\|\mathbf{H}\|_F^2}(s)$ can be given [19]:

$$M_{\|\mathbf{H}\|_F^2}(s) = \frac{1}{\det(\mathbf{I}_{N_t N_r} + s\mathbf{R})} = \prod_{i=1}^{N_t N_r} \frac{1}{1 + s\lambda_i(\mathbf{R})}, \tag{2.25}$$

where $\det(\mathbf{A})$ is the determinant of $\mathbf{A}$ and $\lambda_i(\mathbf{R})$ $(i = 1, 2, \cdots, N_t N_r)$ is the $i$th eigenvalue of $\mathbf{R}$.

## 2.3   Performance Measures

To characterize the performance of diversity systems in slow and flat fading channels, performance measures, such as the average SER, the average BER, the outage probability, and the AF, are commonly used in the literature [14, 15]. Moreover, for MIMO systems, there are two other key measures, known as diversity gain and coding gain.

### 2.3.1   Average Error Rate

The average error rate is one of the most commonly used performance criteria, which evaluates the effectiveness of different diversity schemes in wireless fading channels. It is obtained by averaging the conditional error probability over the statistics of the fading amplitudes. Many approaches have been proposed to evaluate the average error rates of MIMO systems under different fading assumptions. One of the most popular is the PDF-based approach, which averages the conditional error probability over the PDF of the output signal-to-noise ratio (SNR):

$$\bar{P}_e = \int_0^\infty P_e(\gamma) p(\gamma) \, d\gamma \tag{2.26}$$

where $P_e(\gamma)$ is the conditional probability of error given the output SNR $\gamma$ for a specific modulation scheme and $p(\gamma)$ is the PDF of the output SNR in a specified fading channel.

Due to the difficulties of getting closed-form expressions of the infinite integral, the MGF-based approach has been widely used to evaluate the error rate performance of various coherent diversity schemes recently. The basic idea is to find an exponential-type representation for the conditional probabilities so that the average error rates can be expressed strictly in terms of the MGF of the output SNR [20–23].

## 2.3.2 Outage probability

In addition to the average error rate, outage probability is another standard performance criterion of diversity systems, which is defined as the probability that the instantaneous output SNR $\gamma$ falls below a certain given threshold $\gamma_T$. Outage probability is a useful statistical measure of the radio link performance in the presence of interferences. The outage threshold $\gamma_T$ is determined by many factors, such as the receiver structure and the propagation environment.

The outage probability of a diversity combiner relates to the CDF ($F(x)$) of the combiner output SNR as follows [24]:

$$P(\gamma_T) = P_r(0 \leq \gamma \leq \gamma_T) = F(\gamma_T). \tag{2.27}$$

## 2.3.3 Diversity Gain

Diversity schemes at transmit and/or receive ends provide the receiver with multiple copies (or branches) of the transmitted signal. With the increase in the number of independent branches, the probability that all branches fade simultaneously reduces significantly. Thus diversity techniques stabilize the wireless link which will lead to a reduction of the error rate.

To leverage diversity, the transmitter can send the same symbol across all links. With frequency flat fading across all branches, the receiver gets multiple independently faded versions of the transmit symbol $s$, which are given by

$$y_i = \sqrt{\frac{E_s}{N_t}} h_i s + n_i, \quad i = 1, \cdots, N_t \tag{2.28}$$

11

where $y_i$ is the received signal corresponding to the $i$th diversity branch, $E_s/N_t$ is the symbol energy available to the transmitter for each of the $N_t$ diversity branches, $h_i$ is the channel response of the $i$th diversity branch, and $n_i$ is additive ZMCSCG noise with variance $N_0$. The additive noise samples are uncorrelated with each other. Given the multiple versions of $s$ at different receive antennas, the SNR $\gamma$ could be maximized by the so-called maximum ratio combining (MRC). Let the average SNR at the receive antenna in a single fading channel be $\eta = E_s/N_0$. Assuming perfect channel knowledge at the receiver, the received SNR $\gamma$ after MRC combiners is given:

$$\gamma = \frac{1}{N_t} \sum_{i=1}^{N_t} |h_i|^2 \eta. \tag{2.29}$$

Using ML detection at the receiver, the probability of symbol error is given by [15]:

$$P_e \approx \overline{N}_e Q\left( \sqrt{\frac{\gamma d_{\min}^2}{2}} \right) \tag{2.30}$$

where $\overline{N}_e$ and $d_{\min}$ are the number of nearest neighbors and the minimum distance of the underlying signal constellation, respectively, and $Q(\cdot)$ denotes the Gaussian Q-function. Applying the Chernoff bound $Q(x) \leq e^{-x^2/2}$, $P_e$ can be upper-bounded by

$$P_e \leq \overline{N}_e e^{-\left( \sum_{i=1}^{N_t} |h_i|^2 \right) \frac{\eta d_{\min}^2}{4N_t}}. \tag{2.31}$$

Averaging the probability of symbol error over the statistics of $h_i$ which are independent ZMCSCG random variables with unit variance, $\overline{P_e}$ is upper-bounded by

$$\overline{P_e} \leq \overline{N}_e \prod_{i=1}^{N_t} \frac{1}{1 + \eta d_{\min}^2/4N_t}. \tag{2.32}$$

In the high SNR region, i.e., $E_s/N_0 \gg 1$, the upper bound can be simplified as

$$\overline{P_e} \leq \overline{N}_e \left( \frac{\eta d_{\min}^2}{4N_t} \right)^{-N_t}. \tag{2.33}$$

Eq. (2.33) relates to the Chernoff upper bound on the probability of the symbol error for the additive white Gaussian noise (AWGN) channel [25]. On a log-log scale, the magnitude

of the slope of the SER versus SNR ($\eta$) curve will demonstrate the effect of diversity. The diversity order is the magnitude of the slope. Diversity gain $G_d$ can be defined as

$$G_d = -\lim_{\eta \to \infty} \frac{\log P_e}{\log(\eta)}.$$ (2.34)

## 2.3.4 Coding Gain

If the average SER $\overline{P}_e$ of an uncoded (or coded) MIMO system at high SNR is approximated by the expression

$$\overline{P}_e \approx c(G_c \cdot \eta)^{-G_d}$$ (2.35)

where $c$ is a scaling constant dependent on the modulation type and the channel statistics, then $G_c$ represents the coding gain, and $G_d$ represents the diversity order. While diversity gain manifests itself in increasing the magnitude of the slope of the error rate curve, coding gain ($G_c$) shifts the error rate curve to the left.

## 2.3.5 Moments

An alternative to the average error rate is to use moments of the output SNR as the performance measures. A single moment, such as the average output SNR alone does not reveal enough information and the higher order moments can furnish additional information for system design. For example, if the variance of the output is small, large fades from the average is not likely. The moments of the combiner output SNR can be obtained by the output MGF ($M(s)$) as

$$m_n = E(\gamma^n) = \int_0^\infty \gamma^n P(\gamma)\,d\gamma = \frac{d^{(n)} M(s)}{ds}\Big|_{s=0}.$$ (2.36)

## 2.3.6 Amount of Fading (AF)

In evaluating the performance of diversity systems, sometimes it is difficult to get closed-form results especially for BER, SER since statistical analysis requires averaging the instantaneous results over the fading distribution. In such cases, a frequently used approach

is to take advantage of the transformed domain (e.g. by its MGF) in order to obtain a computational resolve. The amount of fading (AF), as a measure of the severity of fading, directly utilizes the moments of the fading distribution itself. Thus it becomes a simple but effective way to quantify fading in both single and MIMO systems. For a single channel model, AF is defined by [26, eq. (2)]:

$$AF = \frac{\text{Var}\{\alpha^2\}}{(\mathscr{E}\{\alpha^2\})^2} \tag{2.37}$$

where $\alpha$ is the instantaneous fading amplitude of a complex fading channel, $\text{Var}\{\cdot\}$ is the statistical variance. For a single Rayleigh fading channel, $AF = 1$. In Nakagami-$m$ fading channels, $AF = 1/m$ [18], where the range of the AF is given by the interval $[0, 2]$.

## 2.4   Antenna Selection

The MIMO systems provides higher data rates and the reliability without any additional bandwidth [27]. Higher data rates are achieved by transmitting multiple data streams simultaneously using spatial multiplexing techniques. Increased reliability is achieved by exploiting spatial diversity to significantly reduce the error probability caused by signal fading.

Although MIMO technology has many advantages, they come at the expense of higher hardware cost, higher signal processing complexity, more power consumption, and bigger component size at the transmitter and the receiver. For example every extra transmit/receive antenna pair requires its own dedicated RF chain (power amplifier, low noise amplifier (LNA), analog to digital (A/D) convertors, digital-to-analog convertor (D/A), etc.) [27]. The increase in complexity has inhibited the widespread adoption of MIMO systems. For example, the third-generation cellular system specification (3GPP) currently supports only an optional two antenna space-time transmit diversity scheme and does not require the handsets to have more than one antenna element [28]. Therefore, cost-effective implementation of MIMO technology remains a major challenge. Antenna selection is a possible solution for the complexity drawbacks of MIMO systems. It reduces the hardware com-

plexity of transmitters and receivers by using fewer RF chains than the number of antenna elements. The idea is that, while the antenna elements are typically cheap, the RF chains are considerably more expensive and therefore must be reduced. The transmission/reception is performed through a subset of the available antenna elements, and selection helps in reducing the implementation cost while retaining most of the benefits of MIMO technology [29]. In antenna selection, a subset of the available antenna elements is adaptively chosen by a switch, and only signals from the chosen subset are processed further by the available RF chains.

### 2.4.1   Antenna Selection Scheme

A block diagram representation of antenna selection at the transmitter and the receiver is given in Fig. 2.1.

   An input bit stream is sent through an encoder and modulator. The space-time encoder converts a single bit stream into symbol streams through a proper mapping and then converts the complex symbol vector into $M_t$ parallel streams of symbols. Each of these streams is sent through a RF chain to produce signal for transmission through each transmit antennas. However, the number of RF chains are smaller than transmit antennas (i.e. $M_t \leq N_t$), thus the RF switch chooses the 'best' $M_t$ antennas out of $N_t$. At the receiver, the RF switch chooses the 'best' $M_r$ out of $N_r$ receive antennas ($M_r \leq N_r$). The channel seen by the selected subset of transmit and receive antennas is the sub-matrix $\widetilde{\mathbf{H}} \in \mathscr{C}^{M_t \times M_r}$, which is obtained by selecting the rows and columns of the channel matrix $\mathbf{H}$ that correspond to the selected receive and transmit antennas, where $\mathscr{C}^{m \times n}$ is a $m \times n$-dimensional complex matrix space. There are $\binom{N_t}{M_t}\binom{N_r}{M_r}$ possible sub-matrices of $\mathbf{H}$. The various selection criteria include the system capacity maximization [30, 31], SNR maximization [32], or union-bound on error rate minimization [33]. In this work, we do not propose new criteria or new methods for selecting antennas. Instead, we analyze the performance of such systems.

15
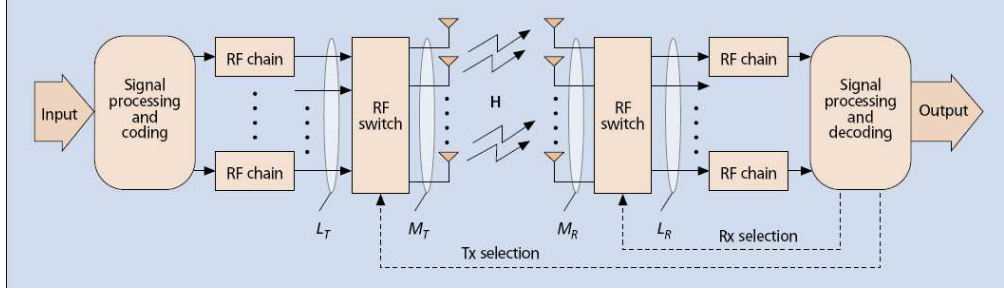
Fig. 2.1. Antenna Selection Scheme

### 2.4.1.1 Receive Antenna Selection (RAS)

Several receive antenna selection (RAS) algorithms to pick the best antenna subset have been proposed [2, 30, 33–36]. Performance analysis for RAS space-time coded systems under both uncorrelated and correlated channels has been reported in [2, 34] where only performance bounds were derived. In [30], Molisch et al. studied the effect of antenna selection from a channel capacity perspective. It was shown that only a small loss in capacity is suffered when the receiver uses a good subset of the available receive antennas.

### 2.4.1.2 Transmit Antenna Selection (TAS)

Just as RAS, TAS is implemented to reduce the complexity at the transmitter. The idea of using transmit diversity is motivated by the difficulty and cost of placing multiple antennas on small mobile handsets. Therefore, multiple antennas are preferably placed at the base station for downlink transmission. Since TAS requires feedback from the receiver side, limited feedback methods are used to improve capacity and performance [37].

TAS has been studied recently. A TAS schematic diagram is given in Fig. 2.2. Joint transmit/receive antenna selection algorithms were presented in [9]. In [38], the authors proposed a new scheme that involves using hybrid selection/maximal-ratio transmission where the transmitter uses a good subset of the available antennas and the receiver uses MRC. They investigated this scheme in terms of SNR, BER, and capacity. They demon-
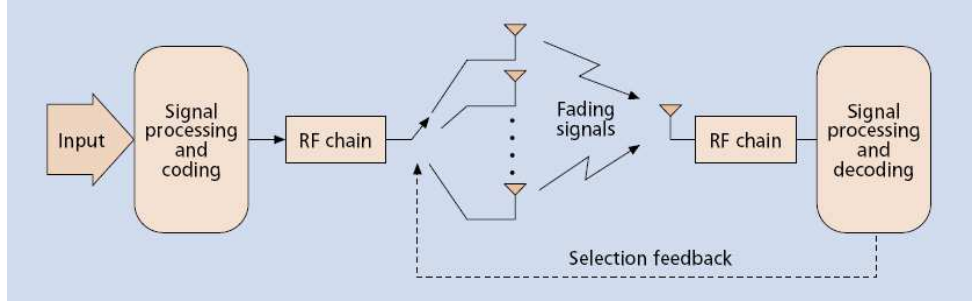
Fig. 2.2. Transmit Antenna Selection Scheme

strated the effectiveness of their scheme relative to already existing schemes. The same scheme was also treated in [39] but the transmitter selects the best single antenna. Other schemes that use hybrid selection/MRC were also considered in [40–43]. A nice overview of antenna selection for MIMO systems can be found in [7].

## 2.4.2 Orthogonal Space-time Block Codes (OSTBCs)

Space-time coding [13, 44] is a coding technique designed for exploiting diversity when multiple transmit antennas are in use. Coding is performed in both spatial and temporal domains to jointly modulate signals transmitted from various antennas at various time periods. The spatial-temporal modulation is used to exploit the MIMO channel fading and to minimize transmission errors at the receiver. Space-time coding can achieve transmit diversity and power gain over spatially un-coded systems without sacrificing the bandwidth [45]. Among all types of space-time codes, space-time block codes with orthogonal designs are the major focus in this thesis.

The Alamouti scheme is the first space-time block code to provide full transmit diversity for systems with two transmit antennas [46]. Tarokh et al. [47] extended the Alamouti's 2-transmit diversity scheme to more than two antennas. A space-time block code is defined by the mapping of the $Q$-tuple input signal $s$ to the set of signals to be transmitted from $M_t$ antennas over $T$ time intervals, represented in a $M_t \times T$ transmission matrix $\mathbf{X}$ as

17

$$\mathbf{X} = \begin{bmatrix} x_{1,1} & x_{1,2} & \cdots & x_{1,T} \\ x_{2,1} & x_{2,2} & \cdots & x_{2,T} \\ \cdots\cdots\cdots\cdots\cdots\cdots\cdots \\ x_{M_t,1} & x_{M_t,2} & \cdots & x_{M_t,T} \end{bmatrix} \tag{2.38}$$

where $x_{i,t}, 1 \le i \le M_t, 1 \le t \le T$ are functions of the $Q$-tuple input sequence and their complex conjugates. At time slot $t$, $x_{i,t}$ is transmitted from antenna $i$. Since $Q$ information symbols are transmitted over $T$ time intervals, the rate of the code is defined as $R_s = Q/T$. If the condition

$$\mathbf{X}\mathbf{X}^H = (\sum_{i=1}^{Q} |s_i|^2)\mathbf{I} \tag{2.39}$$

holds, where $\mathbf{I}$ is the identity matrix, then the code is called an OSTBC. If the channel coefficients are constant over the $T$ symbols, the orthogonality properties of OSTBC allow simple linear ML decoding by decomposing the MIMO enhanced into $Q$ SISO channels.

The OSTBC codeword is formed from a set of $Q$ symbols $s_1, s_2, \cdots, s_Q$ all taken from the same signal constellation. Space-time block codes can be constructed for any type of signal constellation.

## 2.4.3    OSTB-Coded MIMO Systems with Antenna Selection

The MIMO system model with antenna selection employing OSTBC is given in Fig. 2.1. The received signals are expressed as

$$\mathbf{Y} = \sqrt{\frac{E_s}{M_t}}\widetilde{\mathbf{H}}\mathbf{X} + \mathbf{N} \tag{2.40}$$

where the matrix $\mathbf{Y} \in \mathscr{C}^{M_r \times T}$ is the complex received matrix. $\widetilde{\mathbf{H}}$ is a submatrix of $\mathbf{H}$, $\mathbf{X} \in \mathscr{C}^{M_t \times T}$ is the complex transmitted matrix and $\mathbf{N} \in \mathscr{C}^{M_r \times T}$ is the additive noise matrix consisting of i.i.d. entries with zero mean and $N_0$ variance. If we denote a circularly symmetric complex Gaussian variable with mean $\mu$ and variance $\sigma^2$ as $z \sim \mathscr{CN}(\mu, \sigma^2)$, then each element of $\mathbf{N}$ is denoted as $\mathscr{CN}(0, N_0)$. The coefficient $\sqrt{\frac{E_s}{M_t}}$ ensures that the

18

total transmitted power at each receiver is $E_s$ and is independent of the number of transmit antennas.

As shown in [13], if the $Q$ symbols $\{s_1, \cdots, s_Q\}$ with the unit average power are used for transmission, the ML decoder can be simplified to a symbol-by-symbol decoder of the following form:

$$Z_q = \sqrt{\frac{E_s}{M_t}}(\frac{1}{R_s}\|\widetilde{\mathbf{H}}\|_F^2)s_q + n_q, p = 1, \cdots, Q \qquad (2.41)$$

where $n_q \sim \mathcal{CN}(0, \frac{1}{R_s}\|\widetilde{\mathbf{H}}\|_F^2 N_0)$. The OSTBC MIMO system is then equivalent to $Q$ independent SISO systems [32].

## 2.5  Summary

In this chapter, MIMO antenna selection is briefly reviewed. Statistical assumptions, performance measures are introduced. Different antenna selection schemes are summerized, and the general system model with OSTBC is provided.

# Chapter 3

# Amount of Fading Analysis in MIMO Systems with TAS

This chapter is organized as follows. The background is provided in Section 3.1. Section 3.2 introduces the system and the channel model based on order statistics. In Section 3.3, the AF is analyzed for i.i.d. Rayleigh fading channels. By utilizing the Kronecker model, the AF is analyzed for receiver correlation channels in Section 3.4. In Section 3.5, the average SER at high SNR is expressed in terms of the AF. The main results are summarized in Section 3.6.

## 3.1 Introduction

Recently, MIMO TAS systems have received much interest [12, 48–50]. In [48], the authors analyzed the performance of space-time coded MIMO systems with antenna selection by deriving explicit upper bounds on the pairwise error probability (PEP) for quasi-static Rayleigh flat fading. The authors also described code design principles suitable for antenna selection schemes. Zhang et al. [49] proposed a geometrical framework for theoretically analyzing the diversity order achieved by TAS under spatial multiplexing systems. Furthermore, the approach can be used to evaluate the diversity-multiplexing tradeoff in spatial

multiplexing systems with TAS. In [12] and [50], the authors derived the exact BER and capacity expressions for OSTB-coded TAS systems, respectively. However, the aforementioned works provide considerably complex analysis and do not provide insights into the performance of the proposed systems. This motivates our work to use a simpler performance metric known as amount of fading (AF) [51, 52]. The performance measurements such as SER, BER, diversity, and coding gain can also be quantified by the AF measure. In [51], closed-form expressions for the AF of the MIMO diversity systems are given for identically-distributed spatially-correlated Nakagami-*m* fading channels. In [52], the AF is obtained for the output of the equal gain combiner (EGC) in equally correlated fading channels.

In this chapter, we present AF analysis results for both regular MIMO and TAS systems operating on Rayleigh fading channels. Our research is based on the assumption of identically distributed but possibly correlated channels. Rigorous derivation of the AF generally leads to cumbersome results. Therefore in our work, only the methods for deriving the exact AF under different conditions are produced and detailed derivation will be omitted here. Besides that, we provide simple approximations and bounds in order to gain insights into the degree of fading. Lower bounds and upper bounds of the AF are derived under three different fading cases: independent distributed, receiver correlated and generally correlated fading channels. Also, simplified approximations of the AF are derived for both independent distributed and constant-receiver-correlated fading channels. By utilizing the OSTBC for the selected transmit antennas, the lower and upper bounds for the SER at high SNR are derived. An approximate calculation for SER is also given for the independent fading channels, which is more general than [10]. Based on the SER expression, the AF and SER at high SNR are shown to have a simple relationship. With the approximation, the coding gain can be easily obtained for constant correlated fading channels given the AF. Major results are presented in our paper of [53].

## 3.2 Order Statistics and System Model

Suppose there are $n$ independent random variables $X_i, i = 1, 2, \cdots, n$, each having the same PDF $f(x)$ and corresponding CDF $F(x)$. If they are arranged in ascending order of magnitude as $X_{(1)} \leq X_{(2)} \leq \cdots \leq X_{(n)}$, then $X_{(i)}, i = 1, 2, \cdots, n$ is called the $i$-th order statistic. When $X_i$ are i.i.d., the PDF of the $r$-th order statistic is given by [54]:

$$f_{(r)}(x) = \frac{n!}{(r-1)!(n-r)!} f(x) F^{r-1}(x)[1-F(x)]^{n-r} \tag{3.1}$$

and the CDF is

$$F_{(r)}(x) = \sum_{i=r}^{n} \binom{n}{i} F^i(x)[1-F(x)]^{n-i} \tag{3.2}$$

where $\binom{n}{i} = n!/(i!(n-i)!)$.

To perform TAS, $M_t$ antennas are selected out of $N_t$ transmit antennas. Define the random vectors $\mathbf{h}_j = (h_{1j}, h_{2j}, \cdots, h_{N_r j})^T, 1 \leq j \leq N_t$. The corresponding square Frobenius norm of $\mathbf{h}_j$ is $h_j = ||\mathbf{h}_j||_H^2 = \sum_{i=1}^{N_r} |h_{ij}|^2$. $h_j$ are i.i.d. chi-squared variables with $2N_r$ degrees of freedom and the PDF of $h_j$ is given by [15]:

$$f_{h_j}(h) = \frac{1}{(N_r-1)!} h^{N_r-1} e^{-h}, \quad h \geq 0 \tag{3.3}$$

and the CDF is given by

$$F_{h_j}(h) = 1 - e^{-h} \sum_{k=0}^{N_r-1} \frac{h^k}{k!}, \quad h \geq 0. \tag{3.4}$$

We arrange the different $h_j$ in descending order and denote them by $h_{(1)} \geq h_{(2)} \geq \cdots \geq h_{(N_t)}$, where $h_{(j)}$ is the $j$th largest. The $M_t$ selected transmit antennas correspond to the 1 to $M_t$-th largest $h_{(1)}, \cdots, h_{(M_t)}$. Let $\widetilde{\mathbf{H}} = (\mathbf{h}_{(1)}, \mathbf{h}_{(2)}, \cdots, \mathbf{h}_{(M_t)})^T$ represent the $M_t$ selected columns of $\mathbf{H}$. From the theory of order statistics, the joint PDF of $h_{(1)}, h_{(2)}, \cdots, h_{(M_t)}$ is given by [54]:

$$f_{h_{(1)}, \cdots, h_{(M_t)}}(h_1, \cdots, h_{M_t}) = \frac{N_t!}{(N_t - M_t)!} f_{h_1}(h_1) \cdots f_{h_{M_t}}(h_{M_t})(F_{h_{M_t}}(h_{M_t}))^{N_t - M_t}$$

$$= \frac{N_t!}{(N_t - M_t)!\{(N_r-1)!\}^{M_t}} \left( \prod_{j=1}^{M_t} h_j \right)^{N_r-1} \left( e^{-\sum_{j=1}^{M_t} h_j} \right) \left( 1 - e^{-h_{M_t}} \sum_{k=0}^{N_r-1} \frac{h_{M_t}{}^k}{k!} \right)^{N_t - M_t} \tag{3.5}$$

22

where $h_{(1)} \geq h_{(2)} \cdots \geq h_{(M_t)} \geq 0$.

Consider a MIMO system with $N_t$ transmit and $N_r$ receive antennas. Correlation properties can be modeled as the Kronecker product of the transmitter and receiver correlation described in Section 2.1.2, when the receive antenna correlation is the same for all transmit antennas and vice versa [55].

With OSTBC, the output SNR (per symbol) may be written as

$$\gamma = \frac{E_s}{N_0 M_t R_s} \|\widetilde{\mathbf{H}}\|_F^2 = \frac{E_s}{N_0 M_t R_s} C \tag{3.6}$$

where $C = h_{(1)} + \cdots + h_{(M_t)}$. Thus, the selection criterion maximizes the output SNR, i.e., yields the largest received signal power. According to the definition of the AF in Eq. (2.37) and Eq. (3.6), the AF is independent of $\frac{E_s}{N_0 M_t R_s}$ and can be written as

$$\mathrm{AF} = \frac{\mathrm{Var}\{\gamma\}}{(\mathscr{E}\{\gamma\})^2} = \frac{\mathrm{Var}\{C\}}{(\mathscr{E}\{C\})^2}. \tag{3.7}$$

In the remainder of this chapter, $(N_t, M_t; N_r)$ denotes a MIMO system with $M_t$ $(M_t < N_t)$ transmit antennas selected. In contrast, $(N_t; N_r)$ denotes a regular MIMO system without antenna selection, in which all the $N_t$ transmit and $N_r$ receive antennas are used.

## 3.3 AF for i.i.d. Rayleigh Fading Channels

This section analyzes the AF expressions for $(N_t; N_r)$ and $(N_t, M_t; N_r)$ systems when the channel elements $h_{ij}$ are independent of each other. An upper bound, a lower bound and an approximate calculation for AF in $(N_t, M_t; N_r)$ systems are also derived. The results will be verified by simulation.

### 3.3.1 $(N_t; N_r)$ with i.i.d. Rayleigh Fading Channels

With a regular MIMO system (i.e., without antenna selection), the AF may be written as [51] (the case when $m = 1$):

$$AF = \frac{\sum_{i=1}^{N_r N_t} \lambda_i^2}{\left(\sum_{i=1}^{N_r N_t} \lambda_i\right)^2} \tag{3.8}$$

where $\{\lambda_i\}_{i=1}^{N_r N_t}$ are the eigenvalues of the $N_r N_t \times N_r N_t$ channel correlation matrix. When all the channels are independent, the correlation matrix $\mathbf{R}$ reduces to an identity matrix; thus, all the $\lambda_i$ are equal to 1. Therefore, the AF in the i.i.d. case (denoted as $AF_{iid}$) is

$$AF_{iid} = \frac{N_r N_t}{(N_r N_t)^2} = \frac{1}{N_r N_t}. \tag{3.9}$$

### 3.3.2 $(N_t, M_t; N_r)$ with i.i.d. Rayleigh Fading Channels

By using the joint PDF in Eq. (3.5), the general moments of $\mathscr{E}\{h_1^{a_1} \cdots h_{M_t}^{a_{M_t}}\}$ can be calculated as a finite sum (Appendix A). The exact AF in i.i.d. fading channels with TAS can be expressed as

$$AF_{iid\&ts} = \frac{\text{Var}\{(h_1^1 \cdots h_{M_t-1}^0 h_{M_t}^0) + \cdots + (h_1^0 \cdots h_{M_t-1}^0 h_{M_t}^1)\}}{(\mathscr{E}\{(h_1^1 \cdots h_{M_t-1}^0 h_{M_t}^0) + \cdots + (h_1^0 \cdots h_{M_t-1}^0 h_{M_t}^1)\})^2}. \tag{3.10}$$

By expressing the variance as a sum of moments of the form of $\mathscr{E}\{h_1^{a_1} \cdots h_{M_t}^{a_{M_t}}\}$, the AF is expressed as

$$AF_{iid\&ts} = \frac{\mathscr{E}\{(h_1^2 \cdots h_{M_t-1}^0 h_{M_t}^0) + \cdots + (h_1^0 \cdots h_{M_t-1}^0 h_{M_t}^2) + \Sigma_{i,j=1}^L h_i^1 h_j^1\}}{(\mathscr{E}\{(h_1^1 \cdots h_{M_t-1}^0 h_{M_t}^0) + \cdots + (h_1^0 \cdots h_{M_t-1}^0 h_{M_t}^1)\})^2} - 1. \tag{3.11}$$

By using the results in Appendix A, and substituting all the moments into Eq. (3.11), the exact AF can be derived. However, this process is too cumbersome to provide any direct insight.

The AF is a measure of the severity of fading. More generally, the AF is a measure of the randomness of a random variable, so that, the higher the AF, the larger the spread of the fading distribution [56]. Therefore, the more i.i.d. $|h_{ij}|^2$ included in $C$ in Eq. (3.6), i.e., the more randomness contained in $C$, the smaller the AF will be. This result is due to the multiplication of the denominator while the numerator remains largely unchanged. As a

24

result, the AF should decrease with the increasing of the number of the receive antennas $N_r$ and the selected transmit antenna $M_t$. When $M_t$ reaches to the largest $N_t$, the AF reaches the lowest value. Based on the analysis, the upper bound and lower bound of the $AF_{iid\&ts}$ are

$$\frac{1}{N_r N_t} \le AF_{iid\&ts} \le \frac{1}{N_r M_t}. \tag{3.12}$$

Thus, the approximate value of $AF_{iid\&ts}$ (denoted as $AF_{app}$) is given by

$$AF_{app} = \frac{1}{N_r(M_t + (N_t - M_t)\alpha)} \tag{3.13}$$

where $0 \le \alpha \le 1$. When $\alpha = 0$, $AF_{app}$ reaches the lower bound, and when $\alpha = 1$ $AF_{app}$ reaches its upper bound.
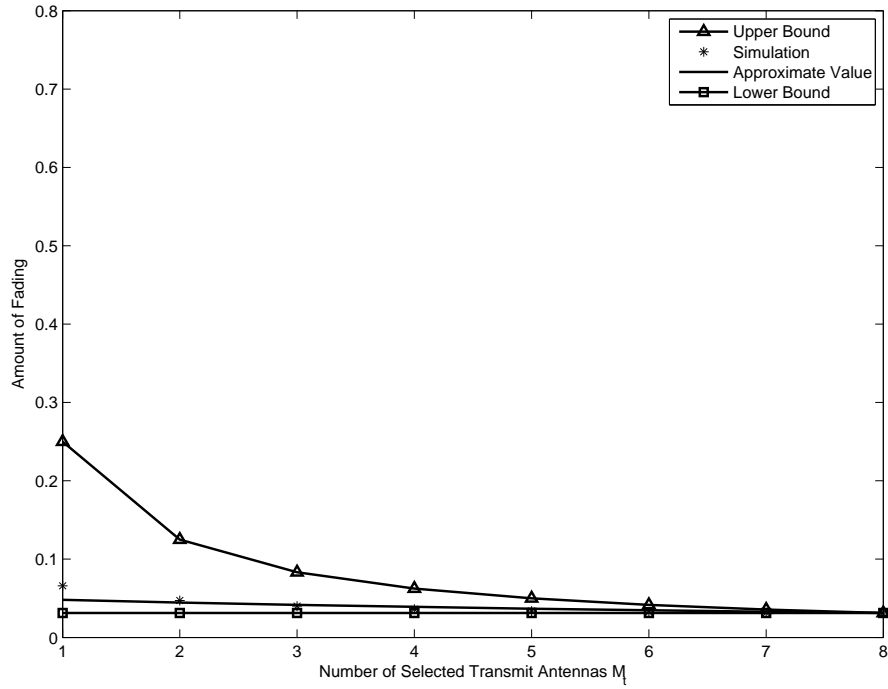


Fig. 3.1. $AF_{iid\&ts}$ for an i.i.d. $(8, M_t; 4)$ system

Fig. 3.1 shows the upper bound, the lower bound and the approximate value for the AF, obtained by using Eq. (3.12) and Eq. (3.13) where setting $\alpha = 0.6$, for MIMO systems with

8 available transmit antennas and 4 receive antennas. The simulation results are shown for comparison. The AF approaches the lower bound when $M_t$ increases, as expected. The AF is closer to the lower bound than to the upper bound. This result shows that antenna selection does not degrade much of the system's behavior in terms of the AF. When $M_t \geq \frac{1}{3}N_t$, the lower bound can be viewed as the approximation of the AF. The values of parameter $\alpha$ are determined for different $N_r$ and $N_t$ in Fig. 3.2. As long as $M_t$ is fixed, $\alpha$ does not change under the same available antenna numbers. Therefore, $M_t$ is set equal to 2. Fig. 3.2 shows that $\alpha$ is smaller for larger $N_t$. This result means that the AF decreases with an increase in the number of the available transmit antennas. When $N_r$ increases above 4, $\alpha$ remains relatively the same.
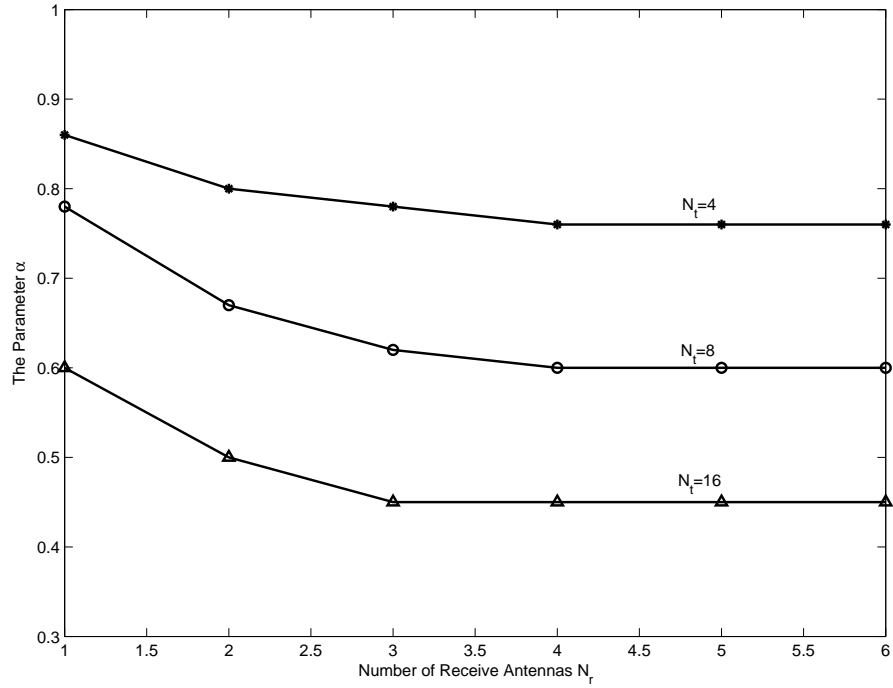


Fig. 3.2. The approximate value of $\alpha$ for different $N_t$ and $N_r$

## 3.4 AF for Fading Channels with Correlation

First consider the case where the channel is correlated only at the receiver side. This correlation implies that the elements within the columns of **H** are correlated but are uncorrelated between columns. Thus, $h_j, 1 \leq j \leq N_t$ are i.i.d.. By utilizing this property, the exact value and bounds for both $(N_r; N_t)$ and $(N_t, M_t; N_r)$ systems are derived. The analysis is extended to the most general case where the correlation exists in both the transmit and receive antennas.

### 3.4.1 $(N_t; N_r)$ with Receiver Antenna Correlation

Under the Kronecker model Eq. (2.24), let $\lambda_i$ $(i = 1, \cdots, N_r N_t)$ denote the eigenvalues of the $N_r N_t \times N_r N_t$ matrix **R**. Then $\lambda_i = \lambda_{t_j} \times \lambda_{r_k}$, where $\lambda_{t_j}$ and $\lambda_{r_k}$ are the eigenvalues for $\mathbf{R}_t$ and $\mathbf{R}_r$, and $i = 1, \cdots, N_r N_t$; $t_j = 1, \cdots, N_r$; $r_k = 1, \cdots, N_t$.

Under the assumption of receive antenna correlation, $\mathbf{R_t}$ is an identical $N_t \times N_t$ matrix, and all $\lambda_{t_j}$ equal 1. Therefore, the $N_r N_t$ of eigenvalues $\lambda_i$ constitute $N_t$ of $\lambda_{r_k}$, i.e., the multiplicity of each $\lambda_i$ is $N_t$. From Eq. (3.8), the AF in the receiver correlation case (denoted as $\mathrm{AF_{rc}}$) can be expressed as

$$\mathrm{AF_{rc}} = \frac{1}{N_t} \frac{\displaystyle\sum_{r_k=1}^{N_r} \lambda_{r_k}^2}{\left(\displaystyle\sum_{r_k=1}^{N_r} \lambda_{r_k}\right)^2}. \tag{3.14}$$

In Appendix B, proof of the lower bound for the AF in the general correlation case $\mathrm{AF_{gc}}$ as $\frac{1}{N_r N_t}$ is given, which is the value for independent $(N_t; N_r)$ systems. This bound is also a lower bound for the specific receiver correlation case analyzed here. The correlation between each column of the **H** decreases the randomness of $C$ in Eq. (3.6) and thus increases the value of the AF. Under the worst correlation scenario, $N_t$ of $\lambda_i$ equals $N_r$ and the other $N_t(N_r - 1)$ eigenvalues equal 0. According to Eq. (3.14), the $\mathrm{AF_{rc}}$ can be upper bounded by $\frac{1}{N_t}$. Therefore, the AF in the receiver correlation case could be upper and lower bounded as

$$\frac{1}{N_r N_t} \leq \text{AF}_{\text{rc}} \leq \frac{1}{N_t}. \tag{3.15}$$

Furthermore, the lower bound can be tightened according to the rank of the receiver correlation matrix. If $r(\mathbf{R}_r) = r_r$, the lower bound can then be expressed by

$$\text{AF}_{\text{rc}} \geq \frac{1}{N_t r_r}. \tag{3.16}$$

Constant correlation is used as the model for the receiver correlation matrix to illustrate the relationship in Eq. (3.15). Constant correlation is applicable for an array of three antennas placed on an equilateral triangle or for closely spaced antennas other than linear arrays [51]. The correlation matrix $\mathbf{R}_r$ can be written as

$$\mathbf{R}_r = \begin{bmatrix} 1 & \rho & \cdots & \rho \\ \rho^* & 1 & \cdots & \rho \\ \multicolumn{4}{c}{\dotfill} \\ \rho^* & \rho^* & \cdots & 1 \end{bmatrix} \tag{3.17}$$

where $\rho$ is the correlation coefficient. Under the constant correlation model, the eigenvalues are given by [51]

$$\lambda_1 = \cdots = \lambda_{N_r - 1} = 1 - \rho$$
$$\lambda_{N_r} = 1 + (N_r - 1) \times \rho. \tag{3.18}$$

For constant correlation at the receiver side of the MIMO link, the $\text{AF}_{\text{rc}}$ is expressible as [51]

$$\text{AF}_{\text{rc}} = \frac{1}{N_t} \frac{1 + |\rho|^2 (N_r - 1)}{N_r}. \tag{3.19}$$

Fig. 3.3 presents the simulation results and inequality Eq. (3.16) of $\text{AF}_{\text{rc}}$ with different $\rho$ in constant receiver correlation, where the channel matrix is assumed fully ranked. Thus Eq. (3.16) is essentially the same as Eq. (3.15). As expected, $\text{AF}_{\text{rc}}$ equals $\frac{1}{N_r N_t}$ when $\rho = 0$ and increases with $\rho$.
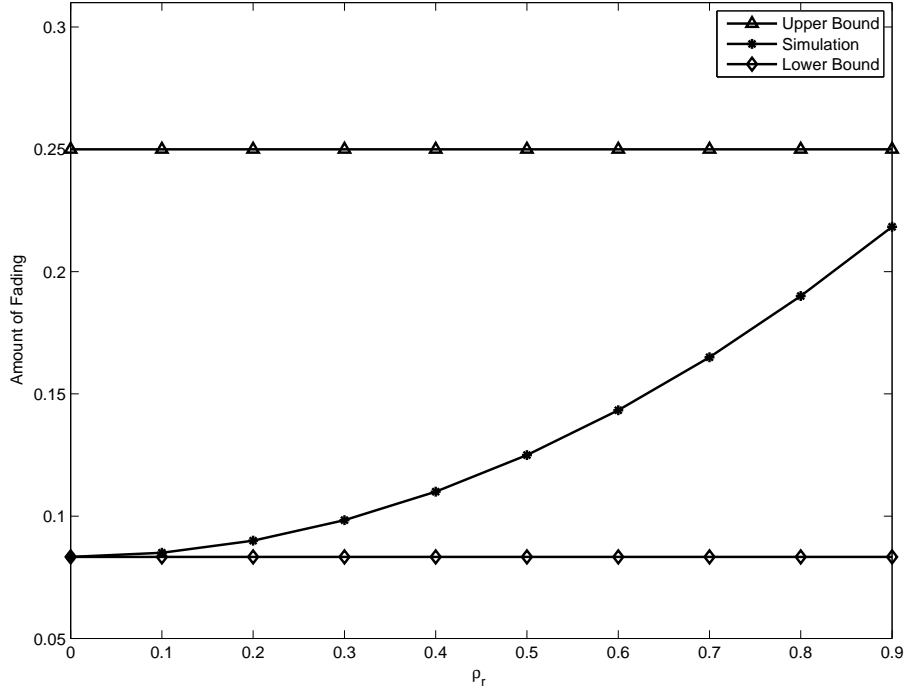
Fig. 3.3. $AF_{\mathrm{rc}}$ with different correlation coefficients in a $(4,3)$ system
with constant receiver correlation

### 3.4.2 $(N_t, M_t; N_r)$ with Receiver Antenna Correlation

Define the receiver correlation matrix $R_r = \mathscr{E}(\mathbf{h}_1, \mathbf{h}_1^H) = \cdots = \mathscr{E}(\mathbf{h}_{N_t}, \mathbf{h}_{N_t}^H)$. The PDF of $\mathbf{h}_{\{j\}}, 0 \leq j \leq M_t$ is given in Appendix C by using the inverse Z transform. The general moments of $\mathscr{E}\{h_1^{a_1} \cdots h_{M_t}^{a_{M_t}}\}$ can be calculated by using a finite sum based on the joint PDF in Eq. (3.5) (see Appendix C for derivation). By following the same procedure as in the $(N_t, M_t; N_r)$ i.i.d. case, the exact AF can be derived by using Eq. (3.11). The exact calculation is again tedious. The approximation and bounds for the AF are thus analyzed first, and the simulation results are given for verification.

The best situation will occur when no correlation exists between the receive antennas, and every antenna is used; thus, the lower bound for the AF in this case is still $\frac{1}{N_r N_t}$. The largest AF occurs when one of $\lambda_{r_k}$ equals $N_r$ and the other $\lambda_{r_k}$ equal 0, i.e., $r(R_r) = 1$. In this situation, the AF reaches an upper bound $\frac{1}{M_t}$ by canceling $N_r$ in the right side of Eq. (3.12).

29

The range for $M_t$ is $[1, N_t]$; thus, we could tighten the upper bound to be $\frac{1}{M_t + (N_t - M_t)\alpha}$, where $0 \leq \alpha \leq 1$. When $\alpha = 1$, the inequality reduces to that for the regular $(N_t; N_r)$ system with the receiver correlation expressed in Eq. (3.15). When $\alpha = 0$, the upper bound corresponds to the worst case of $\frac{1}{M_t}$. Now the AF in the receiver correlation case with the TAS (denoted as $\text{AF}_{\text{rc\&ts}}$) can be bounded by

$$\frac{1}{N_r N_t} \leq \text{AF}_{\text{rc\&ts}} \leq \frac{1}{M_t + (N_t - M_t)\alpha}, \quad 0 \leq \alpha \leq 1. \tag{3.20}$$

Similarly, for the constant correlation model at the receiver side of the MIMO link, the approximation for the AF (denoted as $\text{AF}_{\text{apprc}}$) is given by substituting the right side of Eq. (3.20) into Eq. (3.19):

$$\text{AF}_{\text{apprc}} \approx \frac{1}{M_t + (N_t - M_t)\alpha} \frac{1 + |\rho|^2(N_r - 1)}{N_r}. \tag{3.21}$$

Fig. 3.4 shows the simulation results and approximations of $AF_{\text{rc\&ts}}$ by using Eq. (3.21) with different correlation coefficients in the constant correlation model when $N_t = 4$, $N_r = 3$. The approximation of the AF in the worst case (when $\rho = 1$) is well bounded by the upper bound. As with the case of $(N_t; N_r)$, the AF also increases with $\rho$ when $M_t$ is fixed. This result again shows that the AF illustrates the severity of fading.

The analysis for the case with correlation at the transmit side and no correlation at the receiver side is similar to that for the derivation above. The bounds for the AF have similar forms simply substituting $N_r$ for $N_t$.

### 3.4.3 $(N_t, N_r)$ and $(N_t, M_t; N_r)$ with general correlation

In the most general case, the channel is correlated at both the transmitter and the receiver. The AF can be calculated from Eq. (3.7). The lower bound is also $\frac{1}{N_r N_t}$, which is the best situation for all cases. Since the AF increases with the correlation severity, the AF can be bounded as

$$\frac{1}{N_r N_t} \leq \text{AF}_{\text{gc}} \leq \text{AF}_{\text{gc\&ts}} \leq 1. \tag{3.22}$$

If $r(\mathbf{R}) = r$ is given, the lower bound can also be tightened:

$$\text{AF}_{\text{gc\&ts}} \geq \frac{1}{r}. \tag{3.23}$$

30
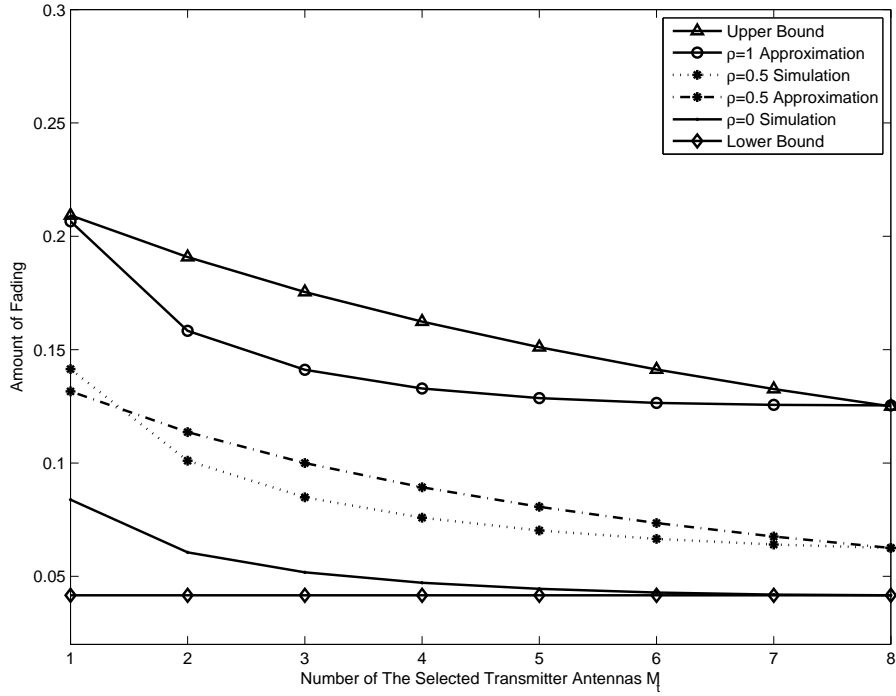
Fig. 3.4. $AF_{\text{rc\&ts}}$ with different correlation coefficients in a $(4, M_t; 3)$ system with constant
receiver correlation                     .

Fig. 3.5 shows how the AF changes with a different $M_t$ and different correlation co-
efficient $\rho$, when both the transmitter and receiver correlations are modeled as constant
correlation. Here, a MIMO system with $N_r = 3, N_t = 4$ is considered. When $\rho$ is less than
0.5, the AF decreases with $M_t$. However, when $\rho$ is larger than 0.5, the more transmit
antennas are selected, the larger the AF is. This result contradicts our intuition that when
the correlation is strong, more transmit antennas are selected, and the system will perform
worse in terms of the index AF. To explain this scenario, there seems to be an optimum
number of antennas to select when the correlation is severe at the transmitter. However, as
assumed, when $M_t$ is fixed, the AF decreases with the numbers of available transmit and
receive antennas.

31
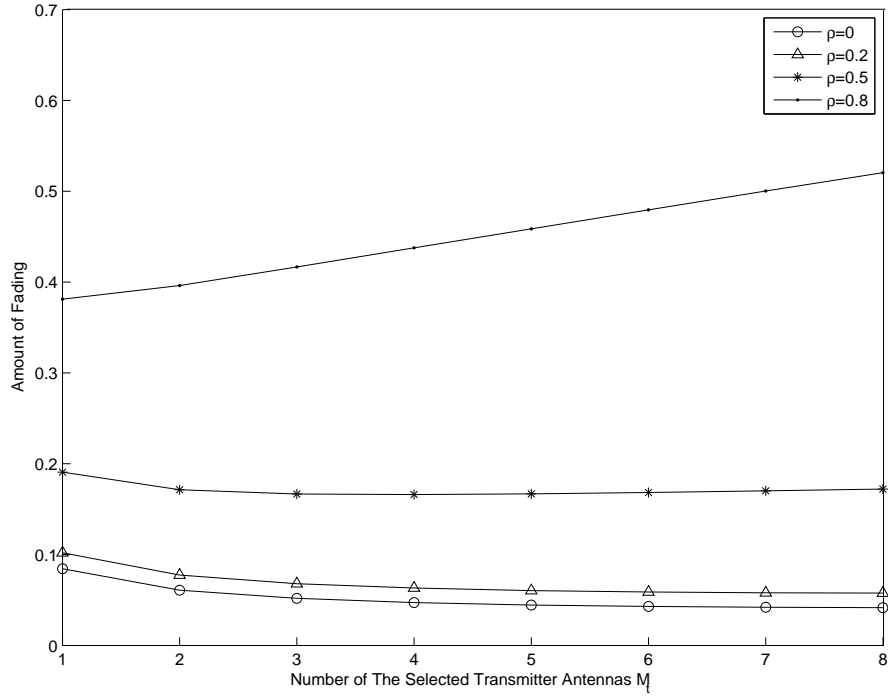
Fig. 3.5. $AF_{\mathrm{gc\&ts}}$ with different $\rho$ in a $(4, M_t; 3)$ system with constant transmit and receiver correlation, $\alpha = 0.4$

## 3.5 Relationship Between AF and the Average SER at High SNR

In this section, the average SER at high SNR is derived as a simple expression for an $(N_t, M_t; N_r)$ system operating on i.i.d. Rayleigh fading channels, when the OSTBC is used for the transmission over the $M_t \times N_r$ link. First, the relationship between the AF and the approximate SER is analyzed. As stated in Eq. (2.35), the diversity order determines the slope of the average SER curve at high SNR in the log-log scale, whereas the coding gain determines the shift of the curve in the SNR relative to a benchmark SER curve given by $c(\gamma)^{-G_c}$ [51].

### 3.5.1 $(N_t; N_r)$ with i.i.d. Fading Channels

First, reconsider a $(N_t; N_r)$ system operating on i.i.d. Rayleigh fading channels. The corresponding instantaneous SER is given by Eq. (2.30) assuming an ML receiver is used. Here, $\gamma$ is determined by using Eq. (3.6), making $\widetilde{\mathbf{H}} = \mathbf{H}$. By applying the Chernoff bound, $Q(x) \leq e^{-\frac{x^2}{2}}$, $P_e$ can be expressed as

$$P_e \leq \overline{N}_e e^{-\frac{1}{4N_t R_s} \frac{E_s}{N_0} \|\mathbf{H}\|_F^2}. \tag{3.24}$$

To determine the value of the diversity, the instantaneous SER should be averaged over the statistics of fading $\overline{P}_e = \mathscr{E}\{P_e\}$. Given the correlation matrix $\mathbf{R}$, the MGF of the random variable $\|\mathbf{H}\|_F^2$, denoted as $M_{\|\mathbf{H}\|_F^2}(s)$, is given in Eq. 2.25. The $\overline{P}_e$ can be upper bounded by setting $s = \frac{d_{\min}^2}{4N_t R_s} \frac{E_s}{N_0}$ in Eq. (2.25); that is,

$$\overline{P}_e \leq \overline{N}_e \prod_{i=1}^{r(\mathbf{R})} \left(1 + \frac{d_{\min}^2}{4N_t R_s} \frac{E_s}{N_0} \lambda_i(\mathbf{R})\right)^{-1}. \tag{3.25}$$

As assumed, when channels are i.i.d., all $\lambda_i$ equal 1. Thus, at the high SNR, the $\overline{P}_e$ can be simplified by

$$\overline{P}_e \leq \overline{N}_e \left(\frac{d_{\min}^2}{4N_t R_s} \frac{E_s}{N_0}\right)^{-N_r N_t}. \tag{3.26}$$

Thus, the diversity order $G_d$ equals $N_r N_t$, and the coding gain $G_c$ equals $\frac{d_{\min}^2}{4N_t R_s}$. Compared with Eq. (3.9) in the i.i.d. case, the AF equals the inverse of the diversity order

$$AF_{\text{iid}} = \frac{1}{G_d}. \tag{3.27}$$

### 3.5.2 $(N_t, M_t; N_r)$ with i.i.d. Fading Channels

In a $(N_t, M_t; N_r)$ system the largest $M_t$ of $h_j$ are selected, the following inequality holds:

$$\frac{\|\mathbf{H}\|_F^2}{N_t} \leq \frac{\|\widetilde{\mathbf{H}}\|_F^2}{M_t} \leq \frac{\|\mathbf{H}\|_F^2}{M_t}. \tag{3.28}$$

If Eq. 3.28 is combined with the definition of $\gamma$ in Eq. (3.6), $\gamma$ is bounded by

$$\frac{\|\mathbf{H}\|_F^2}{N_t R_s} \frac{E_s}{N_0} \leq \gamma \leq \frac{\|\mathbf{H}\|_F^2}{M_t R_s} \frac{E_s}{N_0}. \tag{3.29}$$

With the definition of the average SER in Eq. (3.26), the error rate is bounded as

$$\overline{N}_e\left(\frac{d_{\min}^2}{4M_t R_s}\frac{E_s}{N_0}\right)^{-N_t N_r} \leq \overline{P}_e \leq \overline{N}_e\left(\frac{d_{\min}^2}{4N_t R_s}\frac{E_s}{N_0}\right)^{-N_t N_r}. \tag{3.30}$$

This result clearly shows that the $(N_t, M_t; N_r)$ system can achieve full diversity as in $(N_t; N_r)$ although only part of the transmit antennas are selected for transmission. As $1 \leq M_t \leq N_t$, the $\overline{P}_e$ is approximated as

$$\overline{P}_e \approx \overline{N}_e\left(\frac{d_{\min}^2}{4R_s(M_t + (N_t - M_t)\beta)}\frac{E_s}{N_0}\right)^{-N_t N_r} \tag{3.31}$$

where $0 \leq \beta \leq 1$. That is, the coding gain is approximated as $G_c \approx \frac{1}{M_t + (N_t - M_t)\beta}\frac{d_{\min}^2}{4R_s}$. Compared with the $AF_{\text{iid\&ts}}$ for the $(N_t, M_t; N_r)$ system under i.i.d. fading channels in Eq. (3.13), the coding gain can also be approximated as a function of the AF:

$$G_c \approx \frac{d_{\min}^2}{4R_s N_r}\text{AF}. \tag{3.32}$$

Fig. 3.6 shows the upper bound, the lower bound and the approximate value of SER, obtained by using Eq. (3.31) and Eq. (3.32), compared to the simulation results from using the Alamouti scheme with a 4-QAM signal constellation when $N_r = 1, N_t = 4$ and $\beta = 0.5$. With the increasing of $N_t$ and $N_r$, the upper bound and the lower bound converge, and the approximate $G_c$ becomes more accurate. When $M_t = N_t$, the upper bound and the lower bound converge to the same value, which can be used as the approximate value for the SER. When only one transmit antenna is selected, the system is a special case of the OSTBC, with $R_s = 1$ and $M_t = 1$.

Fig. 3.7 compares the average SER with the coding gain given by Eq. (3.31) and Eq. (3.32) with $N_t = 4$, $N_r = 1$ and $M_t = 1, 3$, respectively. The simulation results of the average SER are also shown as a reference. The diversity order of both cases is 4. Thus, the diversity order depends on the number of the available antennas at the transmitter side and not on the number of the antennas selected. In both figures, the approximations Eq. (3.31) and Eq. (3.32) overlap with the simulation results in the large SNR. Thus, a simple relationship between the AF and coding gain is achieved by Eq. (3.32) in the high SNR region.

34
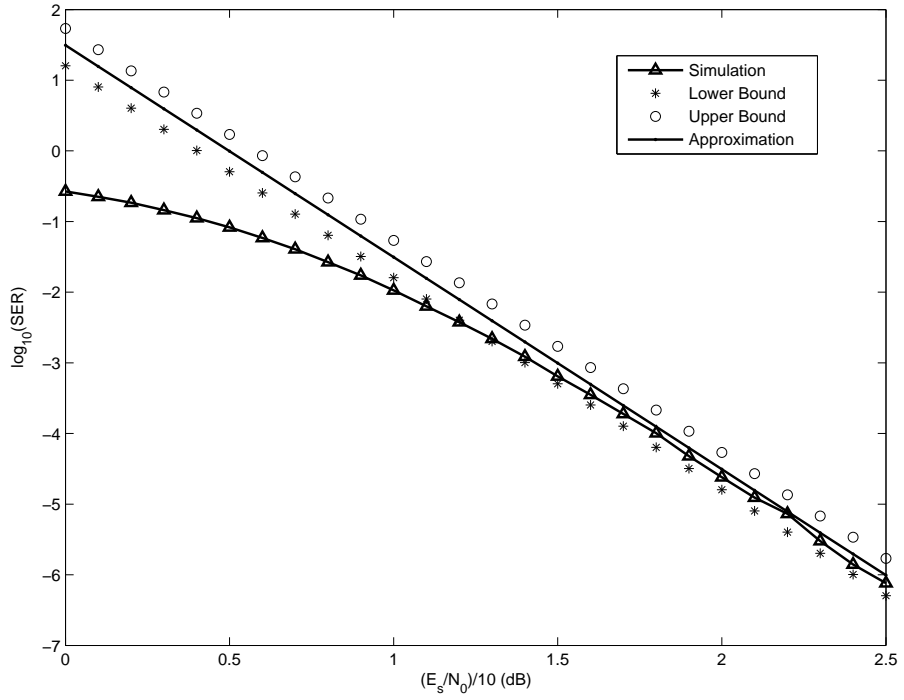
Fig. 3.6. The average SER of 4-QAM using Alamouti Scheme in a (4,2;1) system

### 3.5.3 $(N_t; N_r)$ with Receiver Correlation Fading Channels

In this case, the $\overline{P}_e$ can also be upper bounded by Eq. (3.30). Further, at a high SNR, $\overline{P}_e$ can be simplified to

$$\overline{P}_e \leq \overline{N}_e \left( \frac{d_{\min}^2}{4N_t R_s} \frac{E_s}{N_0} \right)^{-r(\mathbf{R})} \prod_{i=1}^{r(\mathbf{R})} \left( \lambda_i(\mathbf{R}) \right)^{-1}. \tag{3.33}$$

Under the Kronecker model, the eigenvalues $\lambda_i$ of the correlation matrix $\mathbf{R}$ equal the eigenvalue $\lambda_{r_k}$ of the receiver correlation matrix $\mathbf{R}_r$, and the multiplicity of each eigenvalue is $N_t$. The best situation occurs with no correlation at the receiver side. The worst situation occurs when only one of the $\lambda_{r_k}$ is $N_r$. Thus, the lower bound and the upper bound of $\overline{P}_e$ are provided as

$$\overline{N}_e \left( \frac{d_{\min}^2}{4N_t R_s} \frac{E_s}{N_0} \right)^{-N_t N_r} \leq \overline{P}_e \leq \overline{N}_e \left( \frac{d_{\min}^2}{4N_t R_s} \frac{E_s}{N_0} \right)^{-N_t} N_r^{-N_t}. \tag{3.34}$$

35
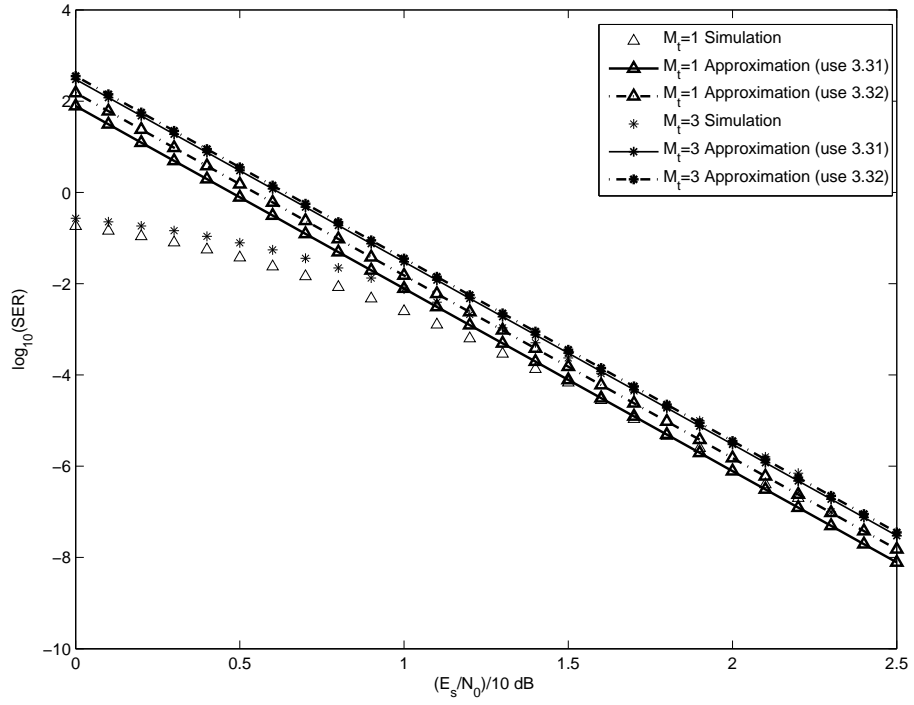
Fig. 3.7. The average SER of 4-QAM with in (4,1;1) and (4,3;1) systems

If $r(\mathbf{R}_r) = r_r$, the lower bound can also be tightened to

$$\overline{P}_e \geq \overline{N}_e \left( \frac{d_{\min}^2}{4N_t R_s} \frac{E_s}{N_0} \right)^{-N_t r_r} \prod_{r_k=1}^{r(\mathbf{R}_r)} \left( \lambda_{r_k}(\mathbf{R}_r) \right)^{-N_t}. \tag{3.35}$$

### 3.5.4 $(N_t, M_t; N_r)$ with Receiver Correlation Fading Channels

Here, the analysis is similar to that in Section 3.4.3 except that the best case will be $M_t = N_t$, and the worst situation occurs when $M_t = 1$. By using Eq. (3.28), the lower bound and the upper bound of $\overline{P}_e$ are

$$\overline{N}_e \left( \frac{d_{\min}^2}{4N_t R_s} \frac{E_s}{N_0} \right)^{-N_t N_r} \leq \overline{P}_e \leq \overline{N}_e \left( \frac{d_{\min}^2}{4M_t R_s} \frac{E_s}{N_0} \right)^{-N_t} N_r^{-N_t}. \tag{3.36}$$

Specially, when the receiver correlation is modeled as a constant correlation, the rank is $N_r$, and the eigenvalue is given in Eq. (3.18). In this case, the average SER can be approximated by

$$\overline{P}_e \approx \overline{N}_e \left( \frac{d_{\min}^2}{4R_s(M_t + (N_t - M_t)\beta)} \frac{E_s}{N_0} \right)^{-N_t N_r} \left( (1 - \rho)^{N_r - 1}(1 + (N_r - 1)\rho) \right)^{-N_t}. \quad (3.37)$$

## 3.6 Conclusion

The AF is a simple measure to quantify the severity of fading. However, exact AF calculations usually involve tedious formulas in TAS systems. In this chapter, the AF of TAS systems under both independent and correlated channels is analyzed. Approximations and bounds are provided for different cases, and a simplified relation between the AF and coding gain is derived. The simulation results show that in the high SNR region, the approximations are accurate.

## 3.7 Appendix A

## General moments for i.i.d. Rayleigh fading channels

The closed-form solution for $\mathscr{E}\{h_1^{a_1} \cdots h_{M_t}^{a_{M_t}}\}$ is now obtained where $a_1, \cdots, a_{M_t}$ are arbitrary indexes. Rewrite the joint PDF in Eq. (3.5) as follows:

$$f_{h_1, \cdots, h_{M_t}}(h_1, \cdots, h_{M_t}) = \frac{N_t!}{(N_t - M_t)!} f_{h_1}(h_1) \cdots f_{h_{M_t}}(h_{M_t})(F_{h_{M_t}}(h_{M_t}))^{N_t - M_t}$$

$$= \frac{N_t!}{(N_t - M_t)!\{(N_r - 1)!\}^{M_t}} (\prod_{j=1}^{M_t} h_j)^{N_r - 1} (1 - e^{h_{M_t}} \sum_{k=0}^{N_r - 1} \frac{h_{M_t}^k}{k!})^{N_t - M_t} \quad (3.38)$$

where $h_1 \geq h_2 \cdots \geq h_{M_t} \geq 0$. Then

$$\mathscr{E}\{h_1^{a_1} \cdots h_{M_t}^{a_{M_t}}\} = \int_0^\infty \int_{h_{M_t-1}}^\infty \cdots \int_{h_2}^\infty h_1^{a_1} \cdots h_{M_t}^{a_{M_t}} f_{h_1, \cdots, h_{M_t}}(h_1, \cdots, h_{M_t}) dh_1 \cdots dh_{M_t}. \quad (3.39)$$

In the first $M_t - 1$ integrals, summations are applied as

$$\int_{h_{i+1}}^\infty h_i^a e^{-bh_i} dh_i = \frac{(a-1)!}{b^a} \sum_{j=0}^a \frac{b^j}{j!} h_{i+1}^j e^{-bh_{i+1}}. \quad (3.40)$$

In the integral with respect to $h_{M_t}$, the following part is binomially expanded:

$$(1 - \sum_{k=0}^{N_r-1} \frac{h_{M_t}{}^k}{k!})^{N_t-M_t} = \sum_{l=0}^{N_t-M_t} (-1)^l \binom{N_t-M_t}{l} e^{lh_{M_t}} \sum_{k=0}^{(N_r-1)l} \beta_{kl} h_{M_t}^k \quad (3.41)$$

where the coefficient $\beta_{kl}$ in Eq. (3.41) is computed by using [57]

$$\beta_{kn} = \sum_{i=k-M_t+1}^{k} \frac{\beta_{i(n-1)}}{(k-i)!} I_{[0,(n-1)(M_t-1)]}(i). \quad (3.42)$$

Here, $\beta_{00} = \beta_{0n} = 1$, $\beta_{k1} = 1/k!$, $\beta_{1n} = n$, and

$$I_{[a,b]}(i) = \begin{cases} 1, & a \le i \le b \\ 0, & \text{otherwise} \end{cases} \quad (3.43)$$

Substituting Eq. (3.38) into Eq. (3.39) and using Eq. (3.41) and Eq. (3.42) we will get:

$$\begin{aligned}
\mathscr{E}\{h_1^{a1} \cdots h_{M_t}^{aM_t}\} &= \frac{(N_t)!}{(N_t-M_t)!((N_r-1)!)^{M_t}} \sum_{i_2}^{i_1+a_1+N_r-1} \sum_{i_3}^{i_2+a_2+N_r-1} \cdots \sum_{i_{M_t}}^{i_{M_t-1}+a_{M_t-1}+N_r-1} \\
&\quad \sum_{l=0}^{N_t-M_t} \sum_{k=0}^{(N_r-1)l} (-1)^l \binom{N_t-M_t}{l} \beta_{kl} \frac{(i_1+a_2+N_r-1)!}{i_2!} \frac{(i_2+a_2+N_r-1)!}{2^{i_2+a_2+N_r} i_3!} \\
&\quad \cdots \frac{(i_{M_t}+a_{M_t-1}+N_r-1)!}{(M_t-1)^{i_{M_t-1}+a_{M_t-1}+N_r} i_{M_t}!} \frac{(i_{M_t}+a_{M_t}+N_r-1)!}{(M_t+l)^{i_{M_t}+a_{M_t}+N_r}}
\end{aligned} \quad (3.44)$$

where $i_1 = 0$. For the special case when $N_r = 1$, Eq. (3.44) can be simplified as

$$\begin{aligned}
\mathscr{E}\{h_1^{a1} \cdots h_{M_t}^{aM_t}\} &= \frac{(N_t)!}{(N_t-M_t)!} \sum_{i_2}^{i_1+a_1} \sum_{i_3}^{i_2+a_2} \cdots \sum_{i_{M_t}}^{i_{M_t-1}+a_{M_t-1}} \sum_{l=0}^{N_t-M_t} \\
&\quad (-1)^l \binom{N_t-M_t}{l} \frac{i_1!}{i_2!} \frac{(i_2+a_2)!}{2^{i_2+a_2+1} i_3!} \\
&\quad \cdots \frac{(i_{M_t}+a_{M_t-1})!}{(M_t-1)^{i_{M_t-1}+a_{M_t-1}+1} i_{M_t}!} \frac{(i_{M_t}+a_{M_t})!}{(M_t+l)^{i_{M_t}+a_{M_t}+1}}.
\end{aligned} \quad (3.45)$$

When $M_t$ reduces to 1, the simplified expression is

$$\mathscr{E}\{h_1^{a1}\} = N_t \sum_{l=0}^{N_t-M_t} (-1)^l \binom{N_t-M_t}{l} \frac{a_1!}{(M_t+l)^{a_1+1}}. \quad (3.46)$$

## 3.8 Appendix B

## The lower bound of AF for correlated Rayleigh fading

Proposition: Assume a Rayleigh fading channel with a general correlation with $N_r$ receive antennas and $N_t$ transmit antennas. The AF could be lower bounded as $\mathrm{AF}_{\mathrm{gc}} \geq \frac{1}{N_r N_t}$.

Proof: For the general correlation, we rewrite Eq. (3.8):

$$\mathrm{AF}_{\mathrm{gc}} = \frac{\sum\limits_{i=1}^{N_r N_t} \lambda_i^2}{\left(\sum\limits_{i=1}^{N_r N_t} \lambda_i\right)^2}. \tag{3.47}$$

Under the assumption of the Knockner model, for the summation of the eigenvalues $\lambda_i$ of the correlation matrix $\mathbf{R}$, we have $\sum_i^{N_r N_t} \lambda_i = N_r \times N_t$. Minimizing the AF reduces to minimizing the numerator of Eq. (3.47). The Lagrange method is used with the condition that $\sum_i^{N_r N_t} \lambda_i = N_r \times N_t$ and

$$V = \lambda_1^2 + \cdots + \lambda_{N_r N_t}^2 - \alpha(\lambda_1 + \cdots + \lambda_{N_r N_t} - N_r \times N_t). \tag{3.48}$$

Partially differentiate $V$ with respect to $\lambda_1, \cdots, \lambda_{N_r N_t}$ and set them to be zero:

$$\frac{\partial V}{\partial \lambda_1} = 2\lambda_1 - \alpha = 0,$$

$$\vdots \tag{3.49}$$

$$\frac{\partial V}{\partial \lambda_{N_r N_t}} = 2\lambda_{N_r N_t} - \alpha = 0. \tag{3.50}$$

The minimal AF is then achieved when $\lambda_1 = \cdots = \lambda_{N_r N_t} = 1$, and the minimum of the AF is $\frac{1}{N_t N_r}$. The proof is complete.

## 3.9 Appendix C

## General moments for receiver-correlated Rayleigh fading channels

The closed-form expression for $\mathscr{E}\{h_1^{a_1}\cdots h_{M_t}^{a_{M_t}}\}$ is obtained when correlation exists at the receiver side. The MGF of $h_j$, where $h_j$ represents the sum of magnitude square of $j$th column of $\mathbf{H}$, can be written as

$$\Phi_{h_j}(s) = E\{e^{-h_j s}\} = \frac{1}{\det\{\mathbf{I}_{m \times m} + \mathbf{R}_r s\}} = \prod_{u=1}^{r_r} \frac{1}{1 + \lambda_u s} \tag{3.51}$$

where $r_r$ is the rank of $\mathbf{R}_r$, $1 \le r_r \le N_r$, and $\lambda_u$ is the eigenvalue of the correlation matrix of the receiver.

By using the inverse Laplace transform of $\Phi_{h_j}(s)$, the PDF of the $h_j$ is given by

$$f_h(t) = \sum_{u=1}^{l} \sum_{v=1}^{r_u} c_{uv} \frac{t^{v-1}}{(v-1)!} e^{-\frac{t}{\lambda_u}}, \quad t > 0. \tag{3.52}$$

Thus, the CDF of $h_j$ is

$$F_h(t) = \sum_{u=1}^{l} \sum_{v=1}^{r_u} \lambda_u^v c_{uv} \cdot \left(1 - e^{-\frac{t}{\lambda_u}} \sum_{k=0}^{v-1} \frac{\left(\frac{t}{\lambda_u}\right)^k}{k!}\right), \quad t > 0 \tag{3.53}$$

where $r_u$ is the multiplicity of each eigenvalue, $r_r = \sum_{u=1}^{l} r_u$, and

$$c_{uv} = \frac{1}{(r_u - v)!} \left\{ \frac{d^{(r_u - v)}}{ds^{(r_u - v)}} [F(s)(s - s_u)^{r_u}] \right\}_{s=s_u}. \tag{3.54}$$

Note that the summation in Eq. (3.52) has a similar form to that of the MGF of a chi-square distribution. By using the same integral as Appendix A, $\mathscr{E}\{h_1^{a_1}\cdots h_{M_t}^{a_{M_t}}\}$ can be written as

$$\mathscr{E}\{h_1^{a_1}\cdots h_{M_t}^{a_{M_t}}\} = \frac{N_t!}{((N_r - 1)!)^{M_t}(N_t - M_t)!} I_1 \cdots I_m \cdots I_{M_t} \tag{3.55}$$

where,

$$I_m = \sum_{u_m=1}^{l} \sum_{v_m=1}^{r_u} \sum_{i_{m+1}=0}^{i_m+v_m+a_1-1} \frac{C_{u_m v_m}}{(v_m - 1)!} \frac{(i_m + v_m + a_1 - 1)!}{(\frac{1}{\lambda_1} + \cdots + \frac{1}{\lambda_m})^{i_m+v_m+a_1} \cdot (i_m + 1)!} \quad 1 \le m \le M_t - 1 \tag{3.56}$$

$$
\begin{aligned}
I_{M_t} &= \sum_{u_{M_t}=1}^{l} \sum_{v_{M_t}=1}^{r_u} \sum_{t=0}^{N_t-M_t} (-1)^t \binom{N_t-M_t}{t} \left( \sum_{u=1}^{l} \sum_{v=1}^{r_u} \lambda_u^v C_{uv} \right)^{N_t-M_t-t} \cdot \sum_{x_1=1}^{l} \sum_{y_1=1}^{r_u} \sum_{z_1=0}^{v_1} \\
&\quad \cdots \sum_{x_t=1}^{l} \sum_{y_t=1}^{r_u} \sum_{z_t=0}^{v_t} \frac{C_{u_{M_t} v_{M_t}} C_{x_1 y_1} \cdots C_{x_t y_t} \lambda_{x_1}^{y_1} \cdots \lambda_{x_t}^{y_t}}{(v_{M_t}-1)! z_1! \cdots z_t!} \\
&\quad \frac{1}{\lambda_{u_1}^{k_1} \cdot \lambda_{u_t}^{k_t}} \frac{(i_{M_t}+v_{M_t}+a_{M_t}+z_1+\cdots+z_t-1)!}{(\frac{1}{\lambda_{u_1}}+\cdots+\frac{1}{\lambda_{u_{M_t}}})^{i_{M_t}+v_{M_t}+a_{M_t}+z_1+\cdots+z_t}}
\end{aligned}
\tag{3.57}
$$

# Chapter 4

# Performance Analysis of T-RAS with OSTBC

This chapter is organized as follows. Overviews of the related literature and the motivation of the proposed work are summarized in Section 4.1. The joint T-RAS system model is briefly described in Section 4.2. An illustrative example is given in Section 4.3 to highlight the difficulties in analyzing the T-RAS systems. The CF for three types of channel models, i.e., Rayleigh, Nakagami-$m$ and Rician, are also given in Section 4.3. Section 4.4 derives the MGF of the output SNR, the average SER, the average BER, outage probability and ergodic capacity. Numerical results are presented to validate the theory and address the effects of various parameters on the BER performance in Section 4.5, followed by conclusions drawn in Section 4.6.

## 4.1   Introduction

Both RAS and TAS have been analyzed in detail. In particular, RAS performance in various channel/correlation models has been comprehensively treated. Among many others, theoretical analysis for generalized selection combining receiver, an RAS scheme, with nonidentical fading was presented in [58]. Other contributions include [59–61]. For TAS,

performance of TAS was analyzed for selecting one antenna at the transmitter in [39]. References [10] and [38] analyzed TAS for Alamouti-coded MIMO systems. The SER and BER of TAS were derived in [11, 12]. The exact capacity expressions were given in [50] for TAS with OSTBCs.

In performance analysis of antenna selection, one needs the statistical distribution of the maximum of a set of branch SNRs or the sum of some of the largest branch SNRs. If the branch SNRs are statistically independent, then those statistics are readily derivable [54]. This is actually the case for both TAS and RAS if the actual channel gains are independent. Consequently, many analytical studies focus on independent fading channels. However, with T-RAS, the branch SNRs are not independent even if the fading channels are i.i.d.. Although order statistics is a well-established branch of statistics, there is surprisingly few available analytical results on correlated random variables [54]. For this reason, the analysis is often made tractable by selection at either the transmitter or receiver – but not both simultaneously [32].

To the best of our knowledge, there is only one paper analyzing T-RAS to date. Cai and Giannakis [62] analyzed error rate performance for selecting one transmit antenna and arbitrary number of receive antennas in independent Rayleigh fading channels. Thus the general problem of analyzing the joint selection of $M_t$ out of $N_t$ transmit antennas and $M_r$ out of $N_r$ receive antennas remains open.

In this chapter, a framework for performance analysis for the general T-RAS for an arbitrary number of transmit and receive antennas is presented. The MIMO channels are not restricted to independent ones but arbitrarily correlated Rayleigh, Nakagami-$m$ or Rician fading channels [15]. The analytical framework introduced for an arbitrarily correlated multi-branch selection combining problem presented in [63] is leveraged to solve the problem. Major work is presented in our paper of [64].

## 4.2 System and Channel Model

A MIMO system with $N_t$ transmit antennas and $N_r$ receive antennas is considered here. The class of OSTBCs provides maximal diversity order in a fading channel and are amenable to low-complexity ML decoding. Assume that the fading channels vary slowly and the feedback delay is sufficiently small to render channel estimation errors negligible, and that the channel state information is perfectly available at the receiver. A subset of $M_t$ transmit antennas and $M_r$ receive antennas is selected and the decision is fed back to the transmitter where OSTBC signal matrices are activated for transmission.

By using OSTBC, the MIMO system is decomposed into several SISO channels as discussed in Section 2.4. In this case, the selection criteria to maximize the channel Frobenius norm will also maximize the received SNR, and thus minimize the probability of error [32].

Now assume that $\widetilde{\mathbf{H}}$ is the actual $M_r \times M_t$ transmission matrix and the received signals can be expressed by Eq. (2.40) as

$$\mathbf{Y} = \sqrt{\frac{E_s}{M_t}} \widetilde{\mathbf{H}} \mathbf{X} + \mathbf{N}. \tag{4.1}$$

To maximize the total received signal power the subset of transmit and receive antennas that yields the largest instantaneous output SNR is selected. There are $N = \begin{pmatrix} N_t \\ M_t \end{pmatrix} \cdot \begin{pmatrix} N_r \\ M_r \end{pmatrix}$ alternates of the selections of transmit and receive antennas. Let $\widetilde{\mathbf{H}}_s$ ($1 \leq s \leq N$) be the $N$ channel sub-matrice corresponding to the $N$ possible antenna subsets. Define $||\widetilde{\mathbf{H}}_s||_F^2 = \sum_{m=1}^{M_r} \sum_{n=1}^{M_t} |h_{i,j}|^2$, where $h_{i,j}$ is the $(m,n)$th element of $\widetilde{\mathbf{H}}_s$ and $1 \leq m \leq M_t, 1 \leq n \leq M_r$. Using an OSTBC, the instantaneous output SNR for each antenna subset can be given by

$$\gamma_s = \frac{E_s}{N_0 R_s M_t} ||\widetilde{\mathbf{H}}_s||_F^2, 1 \leq s \leq N \tag{4.2}$$

where $R_s$ is the symbol rate (symbol/s), $E_s$ is the symbol energy, and $N_0$ is the one-side power spectral density of the white Gaussian noise. The receiver selects antenna subset with maximum instantaneous output SNR expressed by

$$\gamma = \max\{\gamma_1, \cdots, \gamma_N\}. \tag{4.3}$$
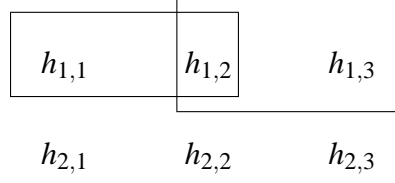
Fig. 4.1. Two possible antenna selection subsets

When the transmitter side receives the selection information, the selected transmit antennas are connected to the available $M_t$ RF chains and the actual transmission occurs through $\widetilde{\mathbf{H}}$.

## 4.3   The CF of T-RAS

In either TAS or RAS, order statistics of independent fading channels can be employed to get the PDF of the output SNR. However even in the case of independent fading channels, all possible subsets of transmit and receive antennas involve correlation, where order statistics of independent variables can no longer be used. First an illustrative example is given.

Consider an MIMO system with 3 available transmit antennas and 2 available receive antennas on independent fading channels and the channel matrix is given in Fig. 4.1. In TAS analysis, the output SNR sent from each transmit antenna is the transmit SNR multiplied by the square norm of each column of the channel matrix $\mathbf{H}$, i.e., as for the first transmitter, $\gamma_1 = (|h_{1,1}|^2 + |h_{2,1}|^2)E_s/N_0$. Arrange $\gamma_i$ where $i = 1, 2, 3$ in descending order and denote them by $\gamma_{(1)} \geq \gamma_{(2)} \geq \gamma_{(3)}$. If $\gamma_1, \gamma_2, \gamma_3$ are i.i.d., the joint or individual PDF of $\gamma_{(s)}$ can be given by order statistics [54]. The SER or BER can be derived based on the known PDF of $\gamma_{(s)}$. On the other hand, the analysis of RAS requires the distribution of sorted output SNRs, the statistics of which can also be obtained similarly.

Now, in generalized T-RAS scheme, if 2 transmit antennas and 1 receive antenna are selected, there are $\binom{3}{2} \cdot \binom{2}{1} = 6$ different choices of antenna subsets. The submatrices of two possible antenna subsets are shown in Fig. 4.3. The left rectangle corresponds to the 1st and

45

2nd transmit antennas and the 1st receive antennas being selected and the output SNR is given by $\gamma_1 = (|h_{1,1}|^2 + |h_{1,2}|^2)E_s/2N_0R_s$. The right rectangle corresponds to selecting the 2nd and 3rd transmit antennas and the 1st receive antennas, where the output SNR is given by $\gamma_2 = (|h_{1,2}|^2 + |h_{1,3}|^2)E_s/2N_0R_s$. The other $\gamma_s$ ($3 \le s \le 6$) are defined similarly. Even if the channels are independent with each other, $\gamma_1$ and $\gamma_2$ are no longer independent since there exists a common term $h_{1,2}$. Thus, the case of T-RAS does not satisfy the condition for the theory of order statistics of independent random variables.

For correlated channels, determination of the statistics of $\gamma_s$ will become even more complicated since the correlation between different $\gamma_s$ will be caused by the common terms as well as the underlying spatial correlation.

To solve this problem, Zhang's analytical framework suggested in a multi-branch selection combining problem [63] is utilized, which expresses the joint PDF of $\gamma_s$ as multiple Fourier transform of its CF. The CDF and PDF of the maximum SNR $\gamma$ among all possible $\gamma_s$ are given by [63, eq. (8)] and [63, eq. (9)]

$$F_\gamma(\gamma) = \frac{1}{(2\pi)^N} \int_{-\infty}^{\infty} \cdots \int_{-\infty}^{\infty} \Phi(t_1, \cdots, t_N) \prod_{s=1}^{N} \frac{1 - e^{-jt_s\gamma}}{jt_s} dt_1 \cdots dt_N \qquad (4.4)$$

and

$$f_\gamma(\gamma) = \frac{1}{(2\pi)^N} \int_{-\infty}^{\infty} \cdots \int_{-\infty}^{\infty} \Phi(t_1, \cdots, t_N) \prod_{s=1}^{N} (jt_s)^{-1}$$
$$\times \sum_{l=1}^{N} (-1)^{l+1} \sum_{b_1 + \cdots + b_N = l} \frac{jT_N}{\exp(j\gamma T_N)} dt_1 \cdots dt_N \qquad (4.5)$$

where $N = \binom{N_t}{M_t} \cdot \binom{N_r}{M_r}$. For brevity, we denote $T_N = b_1 t_1 + \cdots + b_N t_N$ and $b_1, \cdots, b_N$ are binary variables that take values of 0 or 1. In Eq. (4.4), $\Phi(t_1, \cdots, t_N)$ is the joint CF for $\gamma_s$, which solely depends on the channel environment and is independent of the modulation scheme.

In general, the joint CF of the $N$ possible output SNRs $\gamma_s$ is defined as the function [65, eq. (7-50)]

$$\Phi(t_1, \cdots, t_N) = \mathscr{E} \left\{ e^{jt_1\gamma_1 + \cdots + jt_N\gamma_N} \right\} \qquad (4.6)$$

where $\gamma_s$ $(1 \le s \le N)$ are the output SNRs of each possible antenna selection defined in Eq. (4.2). The main difficulty in evaluating Eq. (4.6) is that $\gamma_s$ does not correspond to one single fading channel but related to the $M_t \times M_r$ summation of the square norm of the elements of the $s$th channel matrix $\widetilde{\mathbf{H}}_s$. Thus, the CF for the output SNR $\gamma_s$ in [63] is not suitable for joint antenna selection situation.

In order to overcome this problem, substituting Eq. (4.2) into Eq. (4.6) and we obtain

$$\Phi(t_1, \cdots, t_N) = \mathscr{E} \left\{ e^{aj\left(|h_{1,1}|^2 \Sigma_{k=1}^N c_k t_k + \cdots + |h_{N_r,N_t}|^2 \Sigma_{k=1}^N c_k t_k\right)} \right\} \tag{4.7}$$

where $a = \dfrac{E_s}{N_0 M_t R_s}$ and $c_1, \cdots, c_N$ are binary variables that take values of 0 or 1. The number of the terms in the summation for every $\|h_{i,j}\|^2$ where $c_k = 1$ will be $N_c = \binom{N_t-1}{M_t-1}\binom{N_r-1}{M_r-1}$ and the order of $t_k$ is determined by the arrangement order of different $\gamma_s$. The CF can be obtained by evaluating Eq. (4.7) with respect to $|h_{i,j}|^2$. By using the vectorization of the channel expressed as $\mathbf{h} = \text{vec}[\mathbf{H}]$, Eq. (4.7) can be rewritten as the Hermitian quadratic form of $\mathbf{h}$ as

$$\Phi(t_1, \cdots, t_N) = \mathscr{E} \left\{ e^{\mathbf{h}^H \mathbf{Q} \mathbf{h}} \right\} \tag{4.8}$$

where $\mathbf{Q}$ is the diagonal matrix with the diagonal elements being the coefficients of $|h_{i,j}|^2$ in Eq. (4.7), i.e.,

$$\mathbf{Q} = \text{diag}\left\{ aj \sum_{k=1}^N c_k t_k, \cdots, \sum_{k=1}^N c_k t_k \right\}. \tag{4.9}$$

Notice that the form of $\mathbf{Q}$ depends on the number of the selected and available transmit and receive antennas. Examples will be given later to illustrate how to get the diagonal matrix $\mathbf{Q}$.

## 4.3.1 Rayleigh fading channels

For correlated Rayleigh fading channels, the channel vector $\mathbf{h}$ follows complex Gaussian distribution, $\mathbf{h} \sim \mathscr{CN}(\mathbf{0}, \psi)$, where $\psi$ is the covariance matrix defined by

$$\psi = \frac{1}{2} \mathscr{E}\left[ (\mathbf{h} - \mathscr{E}\{\mathbf{h}\})(\mathbf{h} - \mathscr{E}\{\mathbf{h}\})^H \right]. \tag{4.10}$$

Note that the complex covariance matrix $\psi$ also equals $\psi_I + j\psi_{QI}$, where

$$\psi_I = \psi_Q = \mathscr{E}\big[\,(\mathbf{h}_I - \mathscr{E}\{\mathbf{h}_I\})(\mathbf{h}_I - \mathscr{E}\{\mathbf{h}_I\})^T\,\big]$$

$$\psi_{QI} = -\psi_{IQ} = \mathscr{E}\big[\,(\mathbf{h}_I - \mathscr{E}\{\mathbf{h}_I\})(\mathbf{h}_Q - \mathscr{E}\{\mathbf{h}_Q\})^T\,\big] \qquad (4.11)$$

and $\mathbf{h}_I$ and $\mathbf{h}_Q$ are the vectors composed by the real part and the imaginary part of the channel vector $\mathbf{h}$.

When the variance of each element of $\mathbf{h}$ equals to 1, the covariance matrix equals to correlation matrix $\mathbf{R}$ in Rayleigh fading channels. Note here, the definition of the correlation matrix is the normalized covariance. The MIMO channel correlation matrix $\mathbf{R}$ can be approximated by the Kronecker product of the correlation matrix at the transmitter and the receiver Eq. (2.24). Note that the decomposition does not incorporate the most general case of spatial fading correlation, but yields a reasonable compromise between analytical tractability and validity of the channels model.

Several correlation models are available for different antennas configurations. Specially, constant correlation model may be applicable for closely spaced diversity antennas or three antennas placed on an equilateral triangle. Circular correlation model applies to the case when antennas lying on a circle or four antennas placed on a square. Furthermore, when linear array of antenna elements are equally spaced, exponential correlation can be used [66]. Although these models are good approximations in some cases, in reality the correlation matrix $\mathbf{R}$ can take on any arbitrary Hermitian structure since it depends not only on the transmit and receive antenna array configuration but also on the operating environment, such as the incident angle of the arrival and departure, and the angular spread, etc.

The exponential in Eq. (4.7) can be viewed as the CF of Hermitian quadratic forms in $\mathbf{h}$. From [19] [16, eq.(B-3-14)], the joint CF of output $\gamma_s$ can be derived as

$$\Phi(t_1, \cdots, t_N) = \det(\mathbf{I} - \mathbf{R}\mathbf{Q})^{-1} \qquad (4.12)$$

where $(\cdot)^{-1}$ is the matrix inverse operator. An alternative expression to Eq. (4.12) is obtained by noting that the normalized fading power correlation coefficient $\rho^{\text{power}}$ is the

squared amplitude of the complex channel correlation coefficients in $\mathbf{R}$ [67], i.e., $\rho^{\mathrm{power}}(m,n) = |\mathbf{R}(m,n)|^2$ where $\mathbf{R}(m,n)$ is the $(m,n)$-th element of $\mathbf{R}$. Thus, each element of $\mathbf{R}$ can be taken by the square root of the power correlation coefficients in Eq. (4.12). Therefore, the complex component correlation considered here allows the correlation to be evaluated in terms of the transmit and receive antenna spacing, mean AOA, mean AOD and transmit and receive angular spread. The correlation of the instantaneous power is more convenient for the analysis of experimental data, where they can be easily measured from field data.

Next, the methods to obtain the diagonal matrix $\mathbf{Q}$ in Eq. (4.12) are provided. There are two steps. First, the $N$ output SNR $\gamma_s$ corresponding to the $N$ possible antenna selections are defined in a specific arrangement. Second, the $\gamma_s$s are substituted into the general CF function in Eq. (4.6). The diagonal elements of $\mathbf{Q}$ corresponds to the coefficients of the $|h_{i,j}|^2$. Using the example illustrated before, still consider selecting 2 out of 3 transmit antennas and 1 out of 2 receive antennas, the number of possible antenna selection is $\binom{3}{2}\binom{2}{2} = 6$. If the 6 terms of $\{\gamma_1, \cdots, \gamma_6\}$ is arranged as

$$\gamma_1 = a(|h_{1,1}|^2 + |h_{1,2}|^2), \quad \gamma_2 = a(|h_{1,1}|^2 + |h_{1,3}|^2),$$
$$\gamma_3 = a(|h_{1,2}|^2 + |h_{1,3}|^2), \quad \gamma_4 = a(|h_{2,1}|^2 + |h_{2,2}|^2),$$
$$\gamma_5 = a(|h_{2,1}|^2 + |h_{2,3}|^2), \quad \gamma_6 = a(|h_{2,2}|^2 + |h_{2,3}|^2) \tag{4.13}$$

substituting Eq. (4.13) into Eq. (4.6) the exponential in Eq. (4.6) becomes

$$jt_1\gamma_1 + \cdots + jt_6\gamma_6 = a\{|h_{1,1}|^2 j(t_1 + t_2) + |h_{1,2}|^2 j(t_1 + t_3) + |h_{1,3}|^2 j(t_2 + t_3)$$
$$+ |h_{2,1}|^2 j(t_4 + t_5) + |h_{2,2}|^2 j(t_4 + t_6) + |h_{2,3}|^2 j(t_5 + t_6)\}. \tag{4.14}$$

Thus, the diagonal matrix $\mathbf{Q}$ can be expressed as

$$\mathbf{Q} = \mathrm{diag}\{aj(t_1 + t_2), aj(t_1 + t_3), aj(t_2 + t_3), aj(t_4 + t_5), aj(t_4 + t_6), aj(t_5 + t_6)\}. \tag{4.15}$$

Note that the positions of the diagonal elements of $\mathbf{Q}$ are fixed by the position of $h_{i,j}$ in the channel vector $\mathbf{h}$. With the knowledge of $\mathbf{Q}$, the joint CF for the output SNR $\gamma_s$ of T-RAS can be obtained by Eq. (4.12) with the known correlation matrix $\mathbf{R}$. When the channels are

i.i.d., the joint CF can be expressed by

$$\phi(t_1, \cdots, t_N) = \frac{1}{(1 - a(t_1 + t_2)j)(1 - a(t_1 + t_3)j)(1 - a(t_2 + t_3)j)}$$
$$\times \frac{1}{(1 - a(t_4 + t_5)j)(1 - a(t_4 + t_6)j)(1 - a(t_5 + t_6)j)}. \tag{4.16}$$

## 4.3.2 Nakagami-*m* fading channels

For Nakagami-*m* fading channels, we consider the case when the parameters *m* are equal for all $N_t \times N_r$ channels. Recall Eq. (4.6), the exponential term can be looked as MRC with defining $N_r \times N_t$ output SNRs as $|h_{i,j}|^2$. For arbitrary correlated Nakagami-*m* fading channels with integer *m*, the CF of MRC is obtained by using the central Wishart distribution as [17]

$$\Phi(\omega) = \det(\mathbf{I}_{N_r \times N_t} - j\omega a\frac{\psi}{m})^{-m}, \tag{4.17}$$

where $a = \dfrac{E_s}{N_0 M_t R_S}$ and $\psi$ is the covariance matrix. The variance of each $h_{i,j}$ is *m*. Thus, the $\frac{\psi}{m}$ in Eq. (4.17) equals the correlation matrix **R** and the joint CF of T-RAS can be obtained by setting $\omega = 1$, i.e.,

$$\Phi(t_1, \cdots, t_N) = \det(\mathbf{I} - \mathbf{RQ})^{-\mathbf{m}}, \tag{4.18}$$

where **Q** is the diagonal matrix we showed before. In [17], Luo et al. have shown that for Nakagami-*m* fading channels, the normalized power correlation coefficients is the squared amplitude of the complex channel correlation. Thus, an alternative expression of CF can be obtained by substituting in the square root of the normalized power correlations.

## 4.3.3 Rician fading channels

For correlated Rician fading channels, the channel vector **h** follows the complex Gaussian distribution, $\mathbf{h} \sim \mathscr{CN}(\mu, \psi)$. The mean vector $\mu$ physically represents the direct-path component, whereas the signal strengths of the diffused components are specified by the

diagonal elements of the covariance matrix $\psi$. The Rician factor at the $i$th element of $\mathbf{h}$ can be given by $K_i = \dfrac{|\mu_i|^2}{\psi(i,i)}$ with $\mu_i$ being the $i$th element of $\mu$.

For Rician fading channels, the correlation matrix $\mathbf{R}$, which depicts the correlation between the diffused components, can also be approximate by the Kronecker product of the transmit correlation matrix $\mathbf{R}_t$ and receive correlation matrix $\mathbf{R}_r$ [68]. If the Rician factor $K$ is the same for all channels, the relationship between the covariance matrix $\psi$ and the correlation matrix $\mathbf{R}$ is $\psi = \dfrac{1}{1+K}\mathbf{R}$. When the Rician factor $K$ are different for each fading channels, the relationship of $\psi(i,j)$ and $\mathbf{R}(i,j)$ can be expressed by

$$\psi(i,j) = \frac{1}{\sqrt{(1+K_i)(1+K_j)}}\mathbf{R}(i,j). \tag{4.19}$$

The joint CF of output $\gamma_s$ can be obtained with the help of [19] and given as

$$\Phi(t_1,\cdots,t_N) = \det(\mathbf{I} - \mathbf{RQ})^{-1}\exp\left[\mu^H(\mathbf{Q}^{-1} - \psi)^{-1}\mu\right] \tag{4.20}$$

The Rayleigh fading channel can be treated as a special case of Rician fading with $\mu = 0$ or $K = 0$.

In conclusion, the joint CF depends on two factors. One factor is the channel environment, i.e., the channel model and the channel correlation matrix. The other factor is the numbers of available and selected antennas $(N_t, M_t; N_r, M_r)$ together with the order, which determines the expression of the diagonal matrix $\mathbf{Q}$.

## 4.4   Performance Analysis

With the CF derived in section III, the PDF of the output SNR $\gamma$ of T-RAS can be obtained from Eq. (4.5), which can be further used to evaluate the system performance measurements. In this section, closed-form expressions for the average BER, average SER, outage performance and ergodic capacity are derived for MIMO systems with OSTBC, T-RAS and different modulation formats.

### 4.4.1 BER Analysis

With the knowledge of the PDF of the output SNR $\gamma$ and using Eq. (2.26), the average error rate for a fading wireless system could be obtained as

$$\overline{P}_e = \int_0^\infty P_e(\gamma) f_\gamma(\gamma) d\gamma \tag{4.21}$$

where $P_e(\gamma)$ is the conditional error probability for either BER or SER given instantaneous output SNR $\gamma$. Substituting Eq. (4.5) into Eq. (4.21) yields the average error probability expression

$$\overline{P}_e = \int_0^\infty \cdots \int_0^\infty \Phi(t_1, \cdots, t_N) w(t_1, \cdots, t_N) dt_1 \cdots dt_N \tag{4.22}$$

with

$$w(t_1, \cdots, t_N) = \frac{1}{(2\pi)^N} \int_{-\infty}^\infty P_e(\gamma) \prod_{k=1}^N (jt_k)^{-1} \sum_{l=1}^N (-1)^{l+1} \sum_{b_1+\cdots+b_N=l} \frac{jT_N}{\exp(j\gamma T_N)} d\gamma. \tag{4.23}$$

In Eq. (4.22), the first factor $\Phi(t_1, \cdots, t_N)$ in the integrand is the joint CF of $\gamma_s$ depended solely on the channel characters and the number of antennas. The second factor $w(t_1, \cdots, t_N)$ is the weighting function, which depends only on the modulation scheme. Such a decomposition makes the analysis of error performance systematic. For a given modulation scheme operating in a specified environment, these two factors should be determined and Eq. (4.22) is used to obtain the average error probability.

Consider a MIMO system modulated by $M$-ary square amplitude modulation (M-QAM) with Gray mapping. From [69, 70], the conditional BER can be represented as a sum of $(\sqrt{M} - 1)$ $Q$ functions, expressed by

$$\overline{P}_{e|\text{MQAM}}(\gamma) = \sum_{i=1}^{\sqrt{M}-1} a_i Q(\sqrt{b_i \gamma}) \tag{4.24}$$

where the coefficients $a_i$ and $b_i$ depend on the constellation size $M$. The conditional BER of the binary phase shift keying (BPSK) and binary frequency shift keying (BFSK) can be looked as the special cases of Eq. (4.24) with $M = 2$, $a_1 = 1, b_1 = 2$ and $M = 2$, $a_1 =$

$1, b_1 = 1$, respectively. Inserting Eq. (4.24) into Eq. (4.23) yields (similar to [71, eq,(12)]),

$$w(t_1, \cdots, t_N) = \sum_{i=1}^{\sqrt{M}-1} \frac{a_i}{2(2\pi)^N} \prod_{k=1}^{N} (jt_k)^{-1} \left( 1 + \sum_{l=1}^{N} (-1)^l \sum_{b_1+\cdots+b_N=l} \sqrt{\frac{b_i}{b_i + 2jT_N}} \right).$$

(4.25)

After substituting Eq. (4.25) into Eq. (4.22), the average BER of the MIMO systems with T-RAS and modulated by M-QAM, BPSK, BFSK can be numerically calculated.

## 4.4.2 SER Analysis

By defining $P_e(\gamma)$ in Eq. (4.21) as the conditional symbol error rate on the statistics of the output SNR, the average SER can be derived. Here, the MGF-based approach is used to derive the average SER [72].

From the PDF of $\gamma$ in Eq. (4.5), the MGF of the output SNR can be derived as

$$
\begin{aligned}
M_\gamma(s) &= \int_0^\infty e^{-s\gamma} f_\gamma(\gamma) d\gamma \\
&= \frac{1}{(2\pi)^N} \int_{-\infty}^\infty \cdots \int_{-\infty}^\infty \Phi(t_1, \cdots, t_N) \prod_{k=1}^{N} (jt_k)^{-1} \sum_{l=1}^{N} (-1)^{l+1} \sum_{b_1+\cdots+b_N=l} \frac{jT_N}{l+jT_N} dt_1 \cdots dt_N.
\end{aligned}
$$

(4.26)

Using the MGF of $\gamma$, the average SER of M-PSK, square M-QAM, and M-ary pulse amplitude modulation (M-PAM) can be calculated by

$$\overline{P}_{e|\text{MPSK}}(e) = \frac{1}{\pi} \int_0^{\frac{(M-1)\pi}{M}} M_\gamma \left( \frac{g_{\text{MPSK}}}{\sin^2\theta} \right) d\theta \tag{4.27}$$

$$\overline{P}_{e|\text{MQAM}}(e) = \left( 1 - \frac{1}{\sqrt{M}} \right) \frac{4}{\pi} \int_0^{\frac{\pi}{2}} M_\gamma \left( \frac{g_{\text{MQAM}}}{\sin^2\theta} \right) d\theta$$

$$- \left( 1 - \frac{1}{\sqrt{M}} \right)^2 \frac{4}{\pi} \int_0^{\frac{\pi}{4}} M_\gamma \left( \frac{g_{\text{MQAM}}}{\sin^2\theta} \right) d\theta \tag{4.28}$$

$$\overline{P}_{e|\text{MPAM}}(e) = \frac{2}{\pi} \frac{M-1}{M} \int_0^{\frac{\pi}{2}} M_\gamma \left( \frac{g_{\text{MPAM}}}{\sin^2\theta} \right) d\theta \tag{4.29}$$

where $g_{\text{MPSK}} = \sin^2(\frac{\pi}{M})$, $g_{\text{MQAM}} = 3/2(M-1)$, and $g_{\text{MPAM}} = 3/(M^2-1)$.

### 4.4.3 Outage Probability

The conditional capacity on the output SNR $\gamma$ can be given by [13]

$$C(\gamma) = \log_2(1+\gamma). \tag{4.30}$$

For a given transmission rate $R_T$, the probability that the realized T-RAS can not support $R_T$ with the output SNR $\gamma$ is [71, eq,(15)]

$$
\begin{aligned}
P_{\text{out}}(R_T) &= P\left\{\log_2(1+\gamma) < R_T\right\} = F_\gamma\left(2^{R_T} - 1\right) \\
&= \frac{1}{(2\pi)^N} \int_{-\infty}^{\infty} \cdots \int_{-\infty}^{\infty} \Phi(t_1,\cdots,t_N) \prod_{k=1}^{N} \frac{1 - e^{-jt_k(2^{R_T}-1)}}{jt_k} dt_1 \cdots dt_N.
\end{aligned}
\tag{4.31}
$$

The outage probability expression can be derived in a similar manner with that of BER.

### 4.4.4 Ergodic capacity

The ergodic capacity of a MIMO channel is the ensemble average of the information rate over the distribution of the elements of the channel matrix $\mathbf{H}$ [13]. Conditional capacity is given in Eq. (4.30) and the weighting function is [71, eq,(18)]

$$
w(t_1,\cdots,t_N) = \prod_{k=1}^{N} (jt_k)^{-1} \sum_{l=1}^{N} (-1)^{l+1} \sum_{b_1+\cdots+b_N=l} jT_N\Phi(t_1,\cdots,t_N) \int_0^{\infty} C(\gamma)e^{-j\gamma T_N} d\gamma
\tag{4.32}
$$

where $T_N = b_1 t_1 + \cdots + b_N t_N$ is the same as in Eq. (4.5). The ergodic capacity can be derived by using the same approach as Eq. (4.22).

In general, the calculation of error rate, outage probability and ergodic capacity can not be simplified and relied on numerical methods. Gaussian quadrature integration was suggested in [63].

## 4.5 Numerical Results

In this section, 4-QAM is used for all numerical examples. Fig. 4.2 depicts the simulation and theory results of the average BER in two T-RAS MIMO systems over independent

Rayleigh fading environments. Alamouti codes are employed on the selected transmit antennas. One MIMO system chooses $M_t = 2$ out of 3 transmit antennas and $M_r = 2$ out of 2 receive antennas, and the other chooses $M_t = 2$ out of 3 transmit antennas and $M_r = 1$ out of 2 receive antennas. Integrals in Eq. (4.22) are approximated by using truncated Riemann sum of points with equal space 0.2 between -10 and 10. Extending the summation limits will not get different values since the integrant is highly concentrated within the range $[-8, 8]$. In Fig. 4.2, the derived formulas of both systems match very well with the Monte-Carlo simulation results. The system using both two receive antennas outperforms the MIMO with one receive antenna selected. This again implies the tradeoff between the performance and complexity as in [62].

Fig. 4.3 demonstrates the derived formulas of the average SER in a T-RAS MIMO system where $M_t = 2$ are chosen out of 3 transmit antennas and $M_r = 2$ out of 2 receive antennas. Simulation results are shown to compare with the derived results. The outage probability for this system is shown in Fig. 4.4, where calculation results are obtained by Eq. (4.31). In both figures, the calculated values match well with the simulation results.

The dependence of the bit error performance on the spatial correlation is of interest. The correlation depends on the antenna configuration and the operation environment (i.e., fading model, the spacing of antenna elements, mean AOA, mean AOD, transmit and receive angular spread). A series of numerical results are presented to illustrate the effects of these parameters on the average BER over various fading channels. In the following, a MIMO system choosing $M_t = 2$ out of 3 transmit antennas and $M_r = 2$ out of 2 receive antennas is considered.

### 4.5.1 Correlated Rayleigh fading channels

The transmit correlation matrix $\mathbf{R}_t$ and the receive correlation matrix $\mathbf{R}_r$ are generated by using the practical channel model presented in [68, 73, 74]. The model assumes that there are uniform linear arrays (ULA) at both the transmitter and receiver, and that the angular spectrum at both sides follows a Gaussian distribution. Let us denote the relative antenna

spacing between adjacent antennas as $d_r$ at the receiver and $d_t$ at the transmitter. $d_r$ and $d_t$ are measured in units of wavelengths $\lambda = \frac{c}{f_c}$, where $f_c$ is the center frequency of the narrowband signal. We also define $\bar{\theta}_r$, $\bar{\theta}_t$, $\sigma_r$ and $\sigma_t$ as the mean AOA, mean AOD, receive angle spread and transmit angle spread, respectively. Thus, the actual random AOA ($\theta_r$) and AOD ($\theta_t$) can be expressed by $\theta_r = \bar{\theta}_r + \hat{\theta}_r$ and $\theta_t = \bar{\theta}_t + \hat{\theta}_t$ with $\hat{\theta}_r \sim \mathcal{N}(0, \sigma_r^2)$ and $\hat{\theta}_t \sim \mathcal{N}(0, \sigma_t^2)$. With these definitions, the $(p,q)$th entry of $\mathbf{R_r}$ and $\mathbf{R_t}$ can be given by

$$\mathbf{R}_r(p,q) = \exp\left\{-j2\pi(p-q)d_r\cos(\bar{\theta}_r)\right\}\exp\left\{-\left(\frac{1}{2}(2\pi(p-q)d_r\sin(\theta_r)\sigma_r)\right)^2\right\}$$

$$\mathbf{R}_t(p,q) = \exp\left\{-j2\pi(p-q)d_t\cos(\bar{\theta}_t)\right\}\exp\left\{-\left(\frac{1}{2}(2\pi(p-q)d_t\sin(\theta_t)\sigma_t)\right)^2\right\}. \quad (4.33)$$

The correlation matrix $\mathbf{R}$ is given by the Kronecker product of $\mathbf{R}_t$ and $\mathbf{R}_r$. As mentioned in [68], the correlation function is essentially Gaussian with spread inversely proportional to the product of the antenna spacing and angle spread. This agrees with the intuition that smaller antenna spacing or angle spreads will generally lead to higher level of spatial correlation. Substituting the correlation matrix $\mathbf{R}$ and the diagonal matrix $\mathbf{Q}$ (depends on the number of selected and available transmit and receive antennas) into the CF Eq. (4.18) and the average BER Eq. (4.22), the effects of the parameters on the average BER in correlated Rayleigh fading channels can be observed.

Fig. 4.5 illustrates the effect of transmit antenna spacing $d_t$ on the average BER with fixed receive antenna spacing $d_r = 1/5\lambda$ and $1/3\lambda$, $\bar{\theta}_r = \bar{\theta}_t = \pi/2, \sigma_r = \sigma_t = \pi/6$ for transmit SNR = 9 dB. Increasing the transmit antenna separation $d_t$ between the transmit antenna elements reduces their correlation and hence improves the bit error performance. However, once the transmit antenna spacing $d_t$ is increased beyond $\lambda$, the BER starts approaching its maximum achievable performance. The systems also benefit from increasing the receive antenna separation.

The effect of angular spread on the bit error performance is also given. Fig. 4.6 shows the average BER versus the transmit angular spread with $d_t = 1$, $d_r = 1/4\lambda$, $\bar{\theta} = \pi/2$ and $\pi/6$, $\bar{\theta}_r = \pi/2$, $\sigma_r = \pi/6$ for transmit SNR = 9 dB. Both BERs decrease noticeably as the transmit angular spread increases but less than $30^o$. The larger the mean AOA is, the better

56

BER performance with the same angular spread will be. If the transmit angular spread is fixed, BER has similar relationship with receive angular spread and mean AOD. All these are consistent with the fact that the correlation is inversely proportional to the angle spread.

## 4.5.2 Correlated Nakagami-*m* fading channels

For Nakagami-*m* fading channels, the influence of the fading index *m* on the average BER is demonstrated. Though how to determine the correlation matrix at the transmit or receiver side are given in literature, to the best of our knowledge, there is no model to describe the general channel correlation $\mathbf{R}$. The correlation matrix used for the Rayleigh distribution is hence borrowed here with fixed correlation coefficients obtained by $d_t = 1$, $d_r = 1/4\lambda$, $\bar{\theta} = \pi/2$ and $\pi/6$, $\bar{\theta}_r = \pi/2$, and $\sigma_r = \pi/6$. For numerical calculation, if the error is less than $10^{-4}$, the spacing of the Riemannn summation should be smaller. Here, the error bit at the transmit SNR = 9 dB and the space decreasing from 0.2 to 0.1 is calculated.

Fig. 4.7 shows the average BER versus the transmit SNR with $m = 0.7, \ 1, \ 2.1$. It is observed that as the fading parameter *m* increases, the average BER decreases as expected since larger *m* implies less severe fading.

## 4.5.3 Correlated Rician fading channels

For brevity, the same model Eq. (4.33) is used to generate the transmit correlation matrix $\mathbf{R}_t$ and receive correlation matrix $\mathbf{R}_r$. The correlation matrix, which depicts the correlation of the diffused component, is also the Kronecker product of $\mathbf{R}_t$ and $\mathbf{R}_r$. If the Rician factor $K$ is the same for all channels, the covariance matrix $\psi = \sqrt{\frac{1}{1+K}}\mathbf{R}$. The *i*th elements of mean vector $\mu_i$ take the value of $\mu_i = \sqrt{\frac{K}{1+K}}\mathbf{R}(i,i)$. By inserting the $\mu$, $\psi$ and the diagonal matrix $\mathbf{Q}$ into Eq. (4.20) the CF can be obtained. The average BER can be calculated by inserting the derived CF and Eq. (4.25) into Eq. (4.22).

Fig. 4.8 illustrates the effect of transmit antenna spacing $d_t$ on the average BER with $d_r = 1/4\lambda, \bar{\theta}_r = \bar{\theta}_t = \pi/2, \sigma_r = \sigma_t = \pi/6$ for transmit antenna SNR = 9 dB and $K = 0, 4,$ 10. As in the Rayleigh fading channels, the system benefits from the increasing of transmit

antenna space. In the figure, a larger Rician factor achieves a better bit error performance. A larger antenna spacing is needed for a smaller Rician factor. The reason is that a large Rician factor corresponds to a large direct-path component.

## 4.6   Conclusion

This chapter presents a framework to analyze the performance of the MIMO systems with generalized transmit and receive antenna selection. The main difficulty is the correlation between the different antenna subsets comes from antenna selection as well as the spatial channel correlation. The problem can be conquered by expressing the PDF of the maximum output SNR as a function of the joint CF of all possible output SNRs. Thus, we derived several PDF-based performance measures, including average BER, average SER, outage probability and ergodic capacity. Numerical examples are given to illustrate the effect of antenna array configuration and the operating environment on the average BER performance through the correlation coefficient. Our framework can be applied in a wide range of channel models, such as correlated Rayleigh, Nakagami-$m$ and Rician fading channels. Furthermore, the conventional RAS and TAS can be calculated as the special cases of T-RAS.

Fig. 4.2. Average BER versus transmit SNR over independent Rayleigh fading channels .

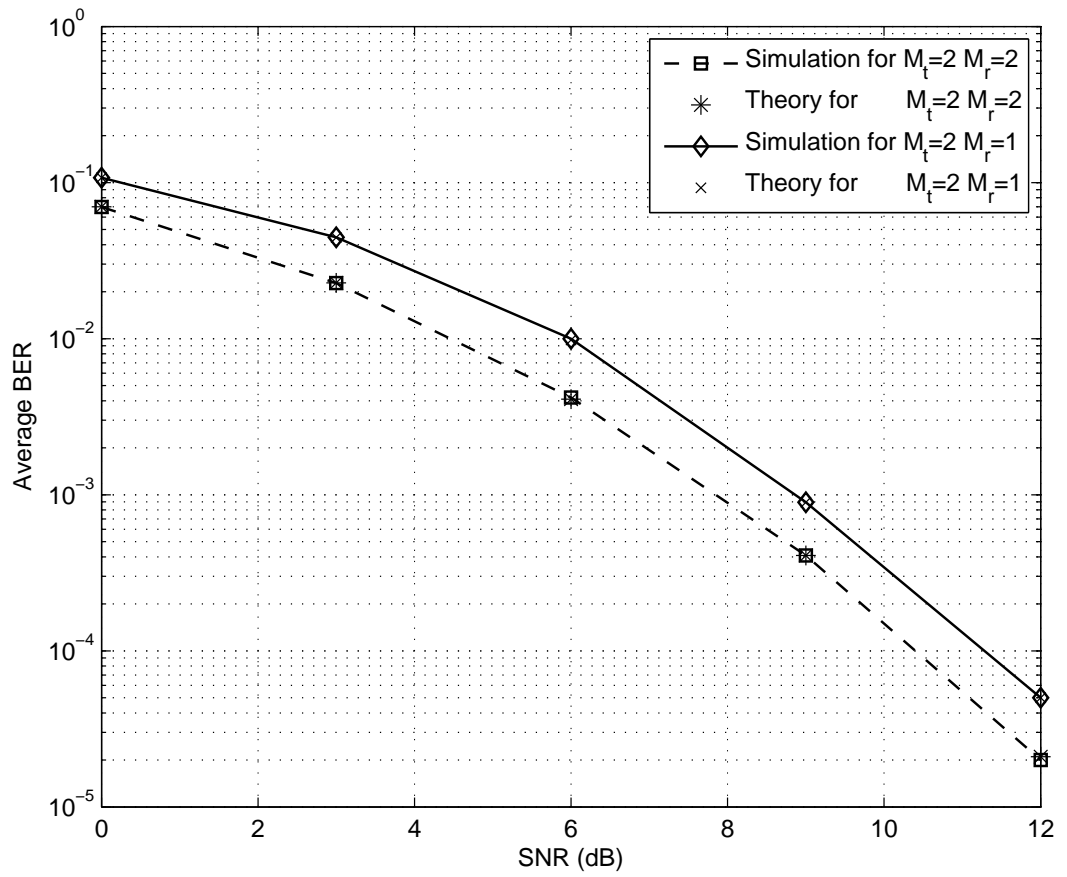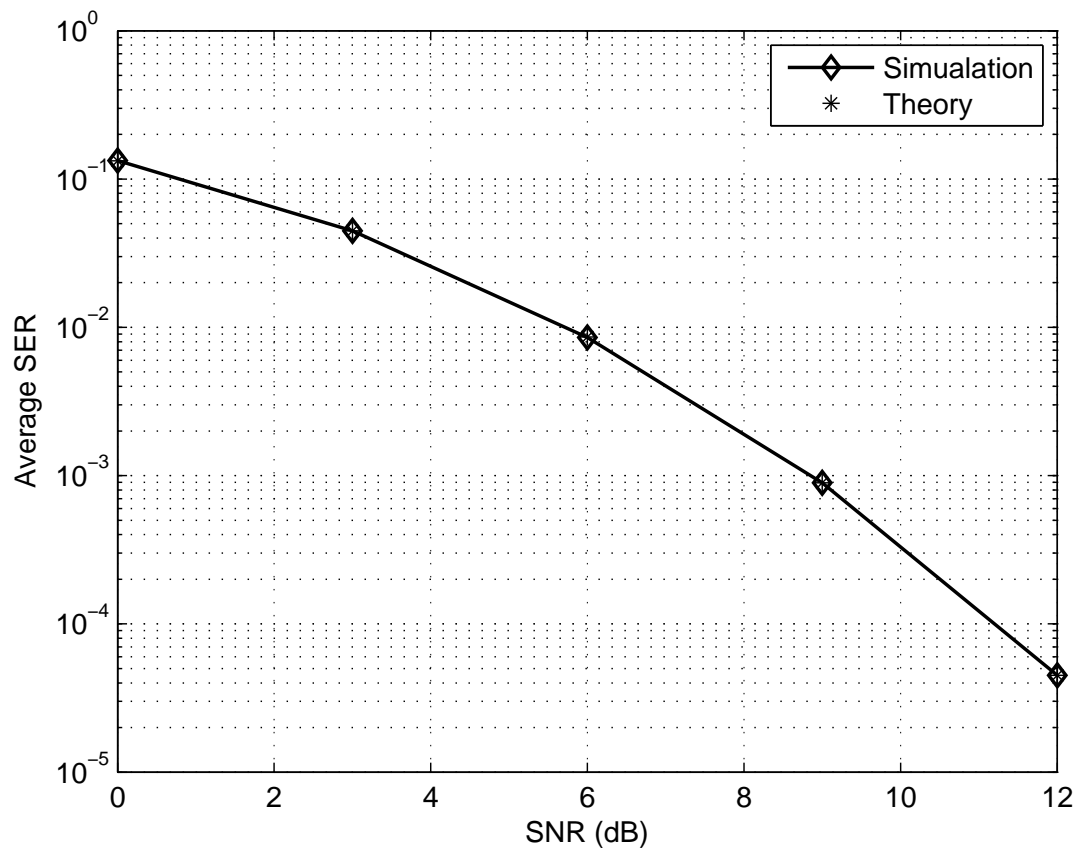Fig. 4.3. Average SER versus transmit SNR over independent Rayleigh fading channels .
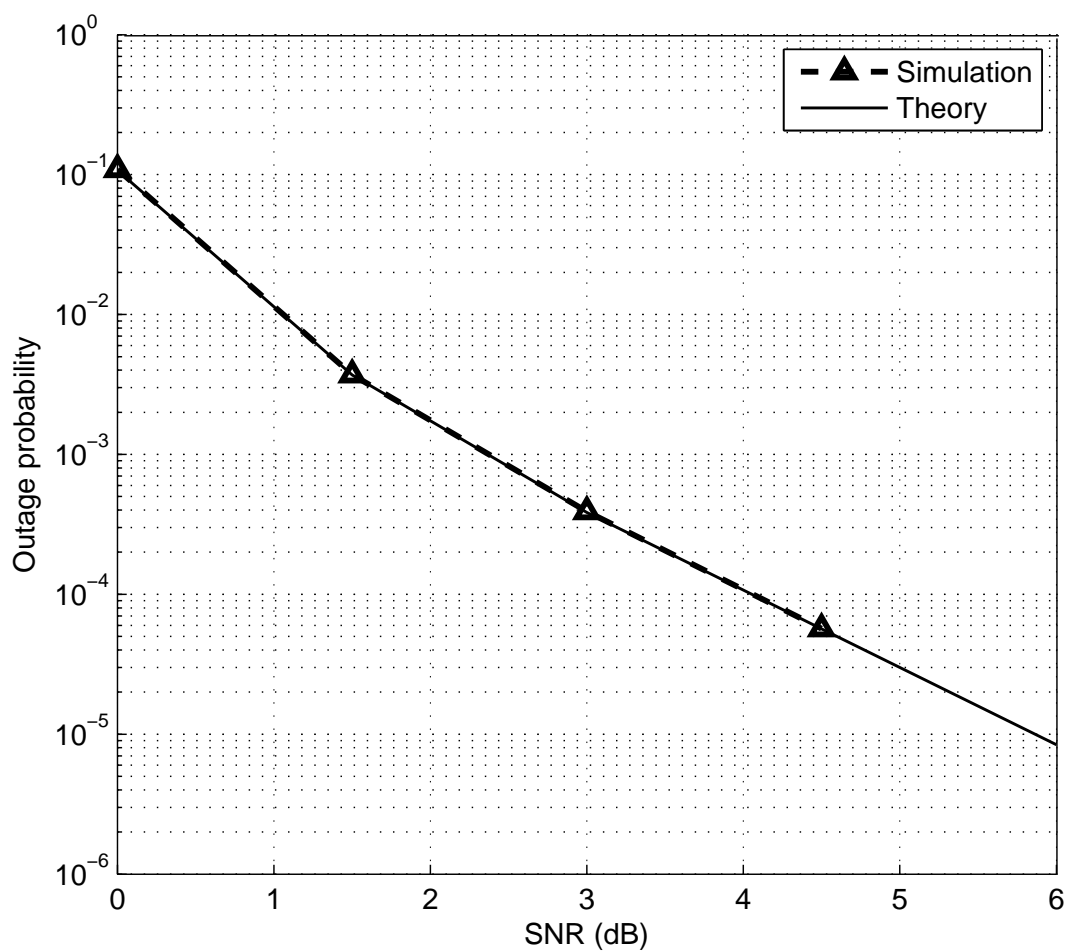
Fig. 4.4. Outage versus transmit SNR over independent Rayleigh fading channels .

61

Fig. 4.5. Average BER versus transmit antenna spacing over correlated Rayleigh fading channels with transmit SNR=9 dB.

Fig. 4.6. Average BER versus transmit angular spread over correlated Rayleigh fading channels with transmit SNR=9 dB.

63

Fig. 4.7. Average BER versus transmit SNR over correlated Nakagami-$m$ fading channels with $m = 0.7, 1, 2.1$.

Fig. 4.8.  Average BER versus transmit antenna spacing over correlated Rician fading channels with transmit SNR=9 dB and $K = 0, 4, 10$.

# Chapter 5

# Conclusions and Future Work
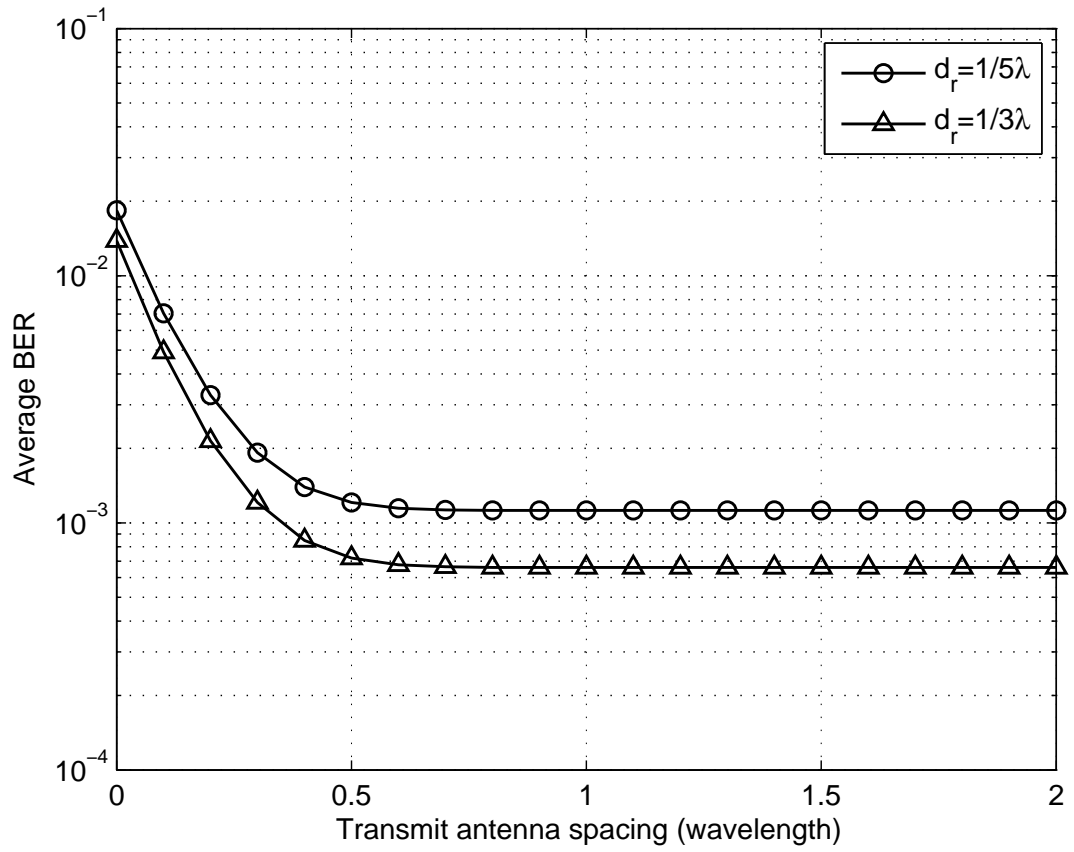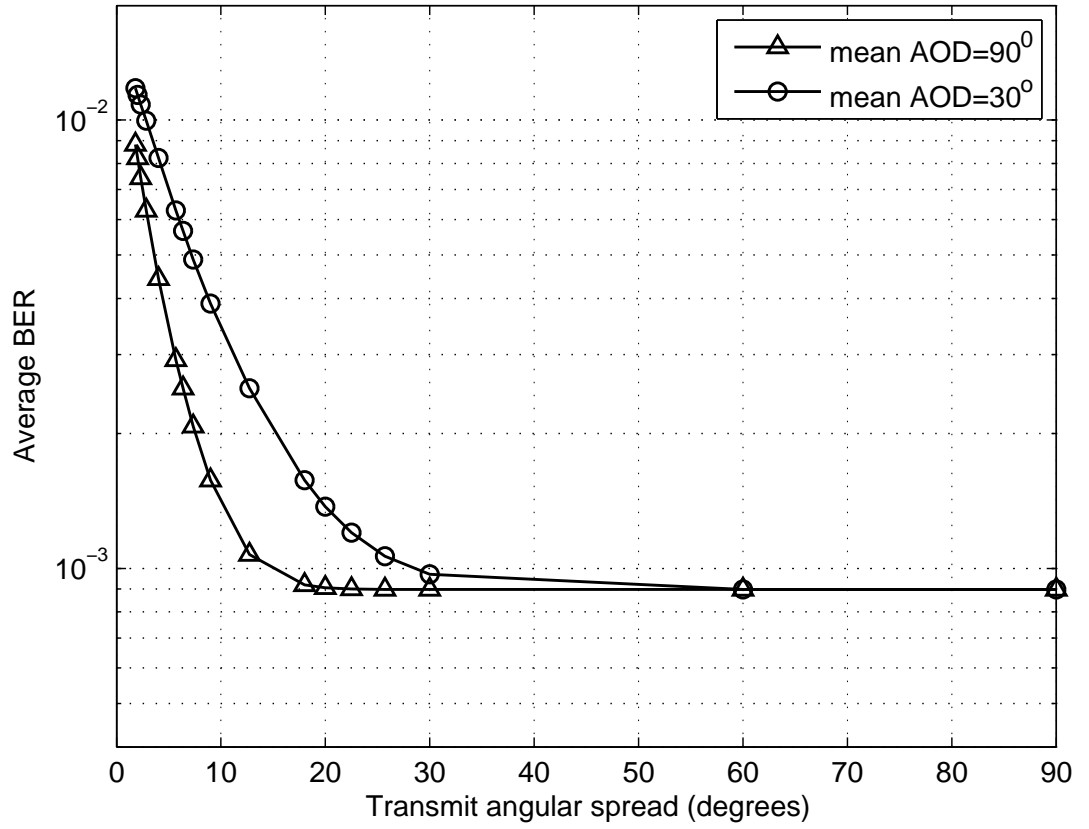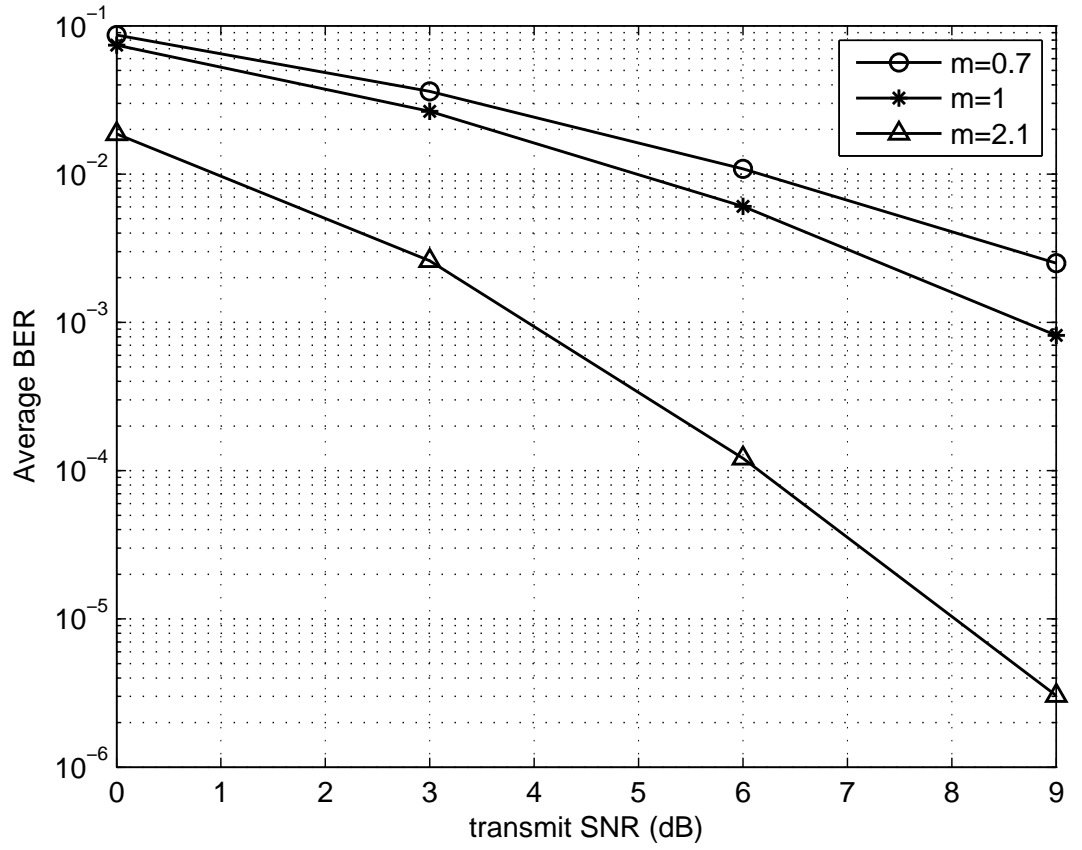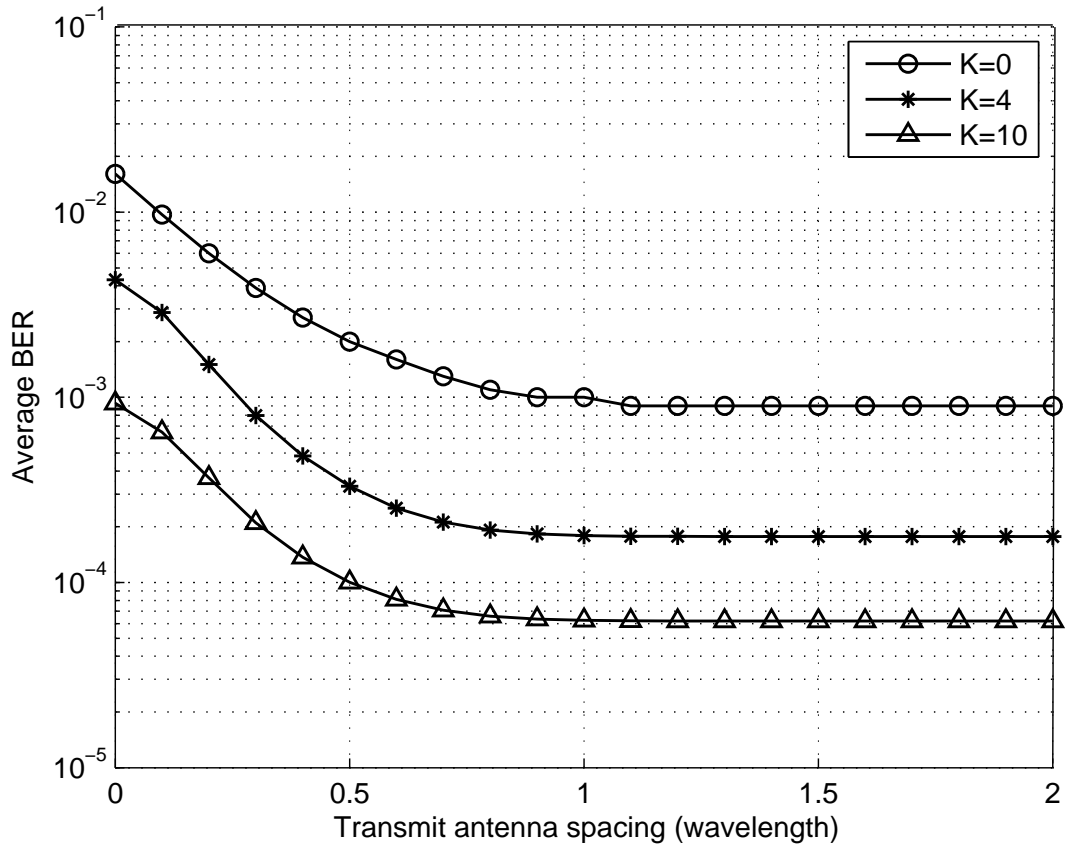
Antenna selection reduces the number of RF chains and consequently reduces the cost as well as the complexity of system without degrading the diversity performance. Therefore, performance analysis of antenna selection is extensively treated, especially under RAS systems. For T-RAS systems, the main difficulty comes from the correlation between the different antenna subsets as well as the original channel correlation. Therefore, many previous work on both TAS and T-RAS systems are limited within independent cases.

In this thesis, the system models of general MIMO and antenna selection schemes are introduced. Different channel assumptions and statistical measures are given in Chapter 2. Research on MIMO systems with antenna selection are reviewed.

In Chapter 3, the AF of TAS systems under both independent and correlated channels is analyzed. We provide approximations and bounds for different cases which could be used as easy references for different fading channels. A simplified relation between the AF and coding gain is derived. The SER can be simply related to the AF for TAS systems with i.i.d. channels. The simulation results show that in the high SNR region, the approximations are accurate.

Chapter 4 introduces a framework to analyze the performance of the MIMO systems with T-RAS. The average BER, average SER, outage probability and ergodic capacity are derived by utilizing the CF of the joint output SNR. This approach can be used not only

on independent but also arbitrarily correlated Rayleigh, Nakagami-*m* and Rician fading channels. Simulation results are provided to validate the numerical calculations. The effect of antenna array configuration and the operating environment (fading, angular spread, mean AOA, mean AOD on the average BER performance are investigated. Both RAS and TAS can be treated as special cases of T-RAS.

Future research topics are as follows:

As an indirect performance measure, AF can offer insights into system performance. However, the analysis of AF under general correlation case is not easily simplified. Also, analysis extended to Nakagami-*m* or rician channels for the most general case of T-RAS could be worked on.

Although the analysis in Chapter 4 could be applied to any antenna selection schemes under any fading channels, possible future work about how to simplify the multi-dimension integral in Eq. (4.22) should be considered. This is useful because the dimension of the integral increases with the number of the selected antennas.

There are other aspects in antenna selection system that could also be considered. For example, in literature performance analysis with imperfect channel estimation is restricted within independent fading cases. To the best of our knowledge, performance analysis with imperfect channel estimation is not given in literature for TAS and T-RAS systems.

# References

[1] A. J. Paulraj, D. A. Gore, R. U. Nabar, and H. Bolcskei, "An overview of MIMO communications - a key to gigabit wireless," *Proc. IEEE*, vol. 92, pp. 198–218, Feb. 2004.

[2] D. Gore, A. Paulraj, "MIMO antenna subset selection with space-time coding," *IEEE Trans. Signal Processing*, vol. 50, pp. 2580–2588, Oct. 2002.

[3] D. Gesbert, M. Shafi, S. Shiu, P. Smith, and A. Naguib, "From theory to practice: An overview of MIMO space-time coded wireless systems," *IEEE J. Select. Areas Commun.*, vol. 21, pp. 281 – 302, Apr. 2003.

[4] J. Winters, "On the capacity of radio communications systems with diversity in Rayleigh fading environments," *IEEE J. Select. Areas Commun.*, vol. 5, pp. 871 – 878, June 1987.

[5] G. Foschini and M. Gans, "On limits of wireless communications in a fading environment when using multiple antennas," *Wirel. Pers. Commun. (Netherlands)*, vol. 6, no. 3, pp. 311 – 335, Mar. 1998.

[6] E. Telatar, "Capacity of multi-antenna Gaussian channels," *European Trans. Telecomm.*, vol. 10, pp. 585 – 595, June 1999.

[7] A. Molisch and M. Win, "MIMO systems with antenna selection," *IEEE Microwave Mag.*, vol. 5, pp. 46 – 56, Mar. 2004.

[8] V. Tarokh, H. Jafarkhani, and A. Calderbank, "Space-time block codes from orthogonal designs," *IEEE Trans. Inform. Theory*, vol. 45, no. 5, pp. 1456 – 1467, July 1999.

[9] S. Sanayei and A. Nosratinia, "Antenna selection in MIMO systems," *IEEE Commun. Mag.*, vol. 42, no. 10, pp. 68 – 73, Oct. 2004.

[10] Z. Chen, J. Yuan, and B. Vucetic, "Analysis of transmit antenna selection/maximal-ratio combining in Rayleigh fading chennels," *IEEE Trans. Veh. Technol.*, vol. 54, no. 4, pp. 1312 – 1321, 2005.

[11] D. Love, "On the probability of error of antenna-subset selection with space-time block codes," *IEEE Trans. Commun.*, vol. 53, pp. 1799 – 1803, Nov. 2005.

[12] S. Kaviani and C. Tellambura, "Closed-form BER analysis for antenna selection using orthogonal space-time block codes," *IEEE Commun. Lett.*, vol. 10, no. 10, pp. 704 – 706, Oct. 2006.

[13] A. J. Paulraj, D. A. Gore, and R. U. Nabar, *Introduction to space-time wireless communications*. Cambridge: Cambridge University Press, 2003.

[14] M. K. Simon and M.-S. Alouini, *Digital Communication over Fading Channels*, 1 ed. New York: Wiley, 2000.

[15] J. G. Proakis, *Digital Communications*, 4 ed. McGraw-Hill, 2001.

[16] M. Schwartz, W. R. Bennett, and S. Stein, *Communication Systems and Techniques*. New York: McGraw-Hill, 1966.

[17] J. Luo, J. Zeidler, and S. McLaughlin, "Performance analysis of compact antenna arrays with MRC in correlated Nakagami fading channels," *IEEE Trans. Veh. Technol.*, vol. 50, no. 1, pp. 267 – 277, Jan. 2001.

[18] M. Nakagami, "The *m*-distribution, a general formula of intensity distribution of rapid fading," in *Statistical Methods in Radio Wave Propagation*, W. G. Hoffman, Ed. Pergamon, Oxford, England, 1960.

[19] G. L. Turin, "The characteristic function of Hermitian quadratic forms in complex normal variables," *Biometrica*, vol. 47, pp. 199–201, June 1960.

[20] M.-S. Alouini and M. K. Simon, "An MGF-based performance analysis of generalized selection combining over Rayleigh fading channels," *IEEE Trans. Commun.*, vol. 48, pp. 401–415, Mar. 2000.

[21] M.-S. Alouini and A. Goldsmith, "A unified approach for calculating error rates of linearly modulated signals over generalized fading channels," *IEEE Trans. Commun.*, vol. 47, no. 9, pp. 1324 – 1334, Sept. 1999.

[22] M.-S. Alouini and M. Simon, "Performance analysis of generalized selective combining over Rayleigh fading channels," in *IEEE Commun. Theory Mini-Conf.*, Vancouver, BC, Canada, 1999, pp. 110 – 114.

[23] M. K. Simon and M. Alouini, "A unified approach to the performance analysis of digital communication over generalized fading channels," *Proceedings of the IEEE*, vol. 86, no. 9, pp. 1860–1877, Sept. 1998.

[24] A. Annamalai and C. Tellambura, "A general approach for evaluating the outage probability in microcellular mobile radio systems," in *Proc. IEEE Int. Conf. Communications (ICC)*, Vancouver, BC, Canada, 1999, vol. 3, pp. 1836–1840.

[25] J. Ventura-Traveset, G. Caire, E. Biglieri, and G. Taricco, "Impact of diversity reception on fading channels with coded modulation. I. Coherent detection," *IEEE Trans. Commun.*, vol. 45, no. 5, pp. 563 – 572, May 1997.

[26] U. Charash, "Reception through Nakagami multipath channels with random delays," *IEEE Trans. Commun.*, vol. 27, no. 4, pp. 657–670, Apr. 1979.

70

[27] N. Mehta and A. Molish, *MIMO System Technology for Wireless Communications*, chapter Antenna Selection in MIMO Systems, pp. 147–173, CRC Press, 2006.

[28] A. Toskala and H. Holma, *WCDMA for UMTS*. New York: John Wiley and Sons, 2002.

[29] A. Gorokhov, D. Gore, and A. Paulraj, *Space-Time Processing for MIMO Communications*, chapter Antenna Subset Selection in MIMO Communication Systems, pp. 147–173, CRC Press, 2006.

[30] A. Molisch, M. Win, and J. Winters, "Capacity of MIMO systems with antenna selection," *IEEE Trans. Wireless Commun.*, vol. 4, no. 4, pp. 1759 – 1771, July 2005.

[31] K. T. Phan and C. Tellambura, "A water-filling algorithm for receive antenna selection based on mutual information maximization," in *Canadian Workshop on Information Theory*, Edmontin, AB, Canada, June 2007, pp. 128–131.

[32] D. Gore and A. Paulraj, "MIMO antenna subset selection with space-time coding," *IEEE Trans. Signal Processing*, vol. 50, no. 10, pp. 2580 – 2588, Oct. 2002.

[33] K. T. Phan and C. Tellambura, "Receive antenna selection for spatial multiplexing systems based on union bound minimization," in *IEEE Wireless Commun. and Networking Conf.*, Hongkong, China, Mar. 2007, pp. 1286–1289.

[34] X. N. Zeng and A. Ghrayeb, "Performance bounds for space-time block codes with receive antenna selection," *IEEE Trans. Inform. Theory*, vol. 50, no. 9, pp. 2130 – 2137, Sept. 2004.

[35] A. Gorokhov, D. Gore, and A. Paulraj, "Receive antenna selection for MIMO flat-fading channels: theory and algorithms," *IEEE Transactions on Information Theory*, vol. 49, no. 10, pp. 2687–2696, Oct. 2003.

[36] J. Heath, S. Sandhu, and A. Paulraj, "Antenna selection for spatial multiplexing systems with linear receivers," *IEEE Commun. Lett.*, vol. 5, no. 4, pp. 142 – 144, Apr. 2001.

[37] R. Blum and J. Winters, "On optimum MIMO with antenna selection," *IEEE Commun. Lett.*, vol. 6, no. 1, pp. 491 – 493, Aug. 2002.

[38] A. Molisch, M. Win, and J. Winters, "Reduced-complexity transmit/receive-diversity systems," *IEEE Trans. Signal Processing*, vol. 51, no. 11, pp. 2729 – 2738, Nov. 2003.

[39] S. Thoen, L. Van der Perre, B. Gyselinckx, and M. Engels, "Performance analysis of combined transmit-SC/receive-MRC," *IEEE Trans. Commun.*, vol. 49, no. 1, pp. 5 – 8, Jan. 2001.

[40] N. Kong and L. Milstein, "Combined average SNR of a generalized diversity selection combining scheme," in *Proc. IEEE Int. Conf. Communications (ICC)*, Atlanta, GA, USA, 1998, vol. 3, pp. 1556 – 1560.

[41] M. Win and J. Winters, "Virtual branch analysis of symbol error probability for hybrid selection/maximal-ratio combining in Rayleigh fading," *IEEE Trans. Commun.*, vol. 49, no. 11, pp. 1926 – 1934, Nov. 2001.

[42] M.-S. Alouini and M. Simon, "Performance of coherent receivers with hybrid SC/MRC over Nakagami-m fading channels," *IEEE Trans. Veh. Technol.*, vol. 48, pp. 1155–1164, July 1999.

[43] A. Annamalai and C. Tellambura, "Analysis of hybrid selection/maximal-ratio diversity combiners with Gaussian errors," *IEEE Trans. Wireless Commun.*, vol. 1, no. 3, pp. 498 – 512, July 2002.

[44] V. Tarokh, N. Seshadri, and A. R. Calderbank, "Space-time codes for high data rate wireless communication: Performance analysis and code construction," *IEEE Trans. Inform. Theory*, vol. 44, pp. 744–765, Mar. 1998.

[45] B. Vucetic and J. Yuan, *Space-time Coding*. New York: John Wiley and Sons, 2003.

[46] S. Alamouti, "A simple transmit diversity technique for wireless communications," *IEEE J. Select. Areas Commun.*, vol. 16, pp. 1451 – 1458, Oct. 1998.

[47] V. Tarokh, H. Jafarkhani, and A. Calderbank, "The application of orthogonal designs to wireless communication," in *IEEE Infor. Theory Workshop*, Killarney, Ireland, June 1998, pp. 46 – 47.

[48] I. Bahceci, T. Duman, and Y. Altunbasak, "Antenna selection for multiple-antenna transmission systems: performance analysis and code construction," *IEEE Trans. Inform. Theory*, vol. 49, no. 10, pp. 2669 – 2681, Oct. 2003.

[49] H. Zhang, H. Dai, Q. Zhou, and B. L. Hughes, "On the diversity order of spatial multiplexing systems with transmit antenna selection: A geometrical approach," *IEEE Transactions on Information Theory*, vol. 52, no. 12, pp. 5297–5311, Dec. 2006.

[50] K. T. Phan and C. Tellambura, "Capacity analysis for transmit antenna selection using orthogonal space-time block codes," *IEEE Commun. Lett.*, vol. 11, no. 5, pp. 423–425, May 2007.

[51] H. Bengt and Geir, "On the amount of fading in MIMO diversity systems," *IEEE Trans. Wireless Commun.*, vol. 4, no. 5, pp. 2498 – 2507, 2005.

[52] Y. Chen and C. Tellambura, "Moments analysis of the equal gain combiner output in equally correlated fading chanels," *IEEE Trans. Veh. Technol.*, vol. 54, no. 6, pp. 1971 – 1979, Nov. 2005.

[53] X. Deng, W. Zhang, and C. Tellambura, "Amount of fading analysis for transmit antenna selection in MIMO systems," in *IEEE Wireless Commun. and Networking Conf.*, Hongkong, China, Mar. 2007, pp. 1161–1165.

[54] H. A. David, *Order statistics*, second ed. New York : Wiley, 1981.

[55] J. Kermoal, L. Schumacher, K. Pedersen, P. Mogensen, and F. Frekeriksen, "A stochastic MIMO radio channel model with experimental validation," *IEEE J. Sel. Areas Commun.*, vol. 20, no. 6, pp. 1211 – 1226, Aug. 2002.

[56] C.-J. Chen and L.-C. Wang, "A unified capacity analysis for wireless systems with joint multiuser scheduling and antenna diversity in Nakagami fading channels," *IEEE Trans. Commun.*, vol. 54, pp. 469 – 478, Mar. 2006.

[57] E. Biglieri, G. Caire, G. Taricco, and J. Ventura-Traveset, "Computing error probabilities over fading channels: A unified approach," *Euro. Trans. Telecommun.*, vol. 9, no. 1, pp. 15–25, Feb. 1998.

[58] A. Annamalai, K. Gautam, and C. Tellambura, "Theoretical diversity improvement in GSC (N,L) receiver with nonidentical fading statistics," *IEEE Trans. Commun.*, vol. 53, pp. 1027–1035, June 2005.

[59] G. Karagiannidis, "Performance analysis of SIR-based dual selection diversity over correlated Nakagami-*m* fading channels," *IEEE Trans. Veh. Technol.*, vol. 52, no. 5, pp. 1207 – 1216, Sept. 2003.

[60] Y. Chen and C. Tellambura, "A new hybrid generalized selection combining scheme and its performance over fading channels," in *IEEE Wireless Commun. and Networking Conf.*, Atlanta, GA, USA, 2004, vol. 2, pp. 926 – 931.

[61] V. A. Aalo and T. Piboongungon, "On the multivariate generalized gamma distribution with exponential correlation," in *IEEE Global Telecommn. Conf. (GLOBECOM)*, St. Louis, Mo, USA, 2005, vol. 5, pp. 1229 – 1233.

[62] X. Cai and G. Giannakis, "Performance analysis of combined transmit selection diversity and receive generalized selection combining in Rayleigh fading channels," *IEEE Trans. Wireless Commun.*, vol. 3, no. 6, pp. 1980 – 1983, Nov. 2004.

[63] Q. Zhang and H. Lu, "A general analytical approach to multi-branch selection combining over various spatially correlated fading channels," *IEEE Trans. Commun.*, vol. 50, no. 7, pp. 1066 – 1073, July 2002.

[64] W. Zhang, C. Tellambura, and X. Deng, "Performance analysis of transmit and receive antenna selection with space-time coding," in *IEEE Global Telecommn. Conf. (GLOBECOM)*, Washington, DC, USA, Nov. 2007.

[65] A. Papoulis, *Probability, random variables, and stochastic processes*, 3 ed. McGraw-Hill, 1991.

[66] M.-S. Alouini, A. Abdi, and M. Kaveh, "Sum of Gamma variates and performance of wireless communication systems over Nakagami-fading channels," *IEEE Trans. Veh. Technol.*, vol. 50, pp. 1471 –1480, Nov. 2001.

[67] J. Luo and J. Zeidler, "A statistical simulation model for correlated Nakagami fading channels," in *Int. Conf. on Commun. Technology*, Beijing, China, 2000, vol. 2, pp. 1680 – 1684.

[68] H. Bolcskei, M. Borgmann, and A. J. Paulraj, "Impact of the propagation environment on the performance of space-frequency coded MIMO-OFDM," *IEEE J. Select. Areas Commun.*, vol. 21, pp. 427 – 439, Apr. 2003.

[69] K. Cho and D. Yoon, "On the general BER expression of one- and two- dimensional amplitude modulations," *IEEE Trans. Commun.*, vol. 50, no. 7, pp. 1074 – 1080, June 2002.

[70] L. Yang and L. Hanzo, "A recursive algorithm for the error probability of M-QAM," *IEEE Commun. Lett.*, vol. 4, no. 10, pp. 304–306, Oct. 2000.

[71] C. K. Au-Yeung and D. J. Love, "A performance analysis framework for limited feedback beamforming in correlated fading," *IEEE Commun. Lett.*, vol. 10, no. 5, pp. 334 – 346, May 2006.

[72] C. Tellambura, A. J. Mueller and V. K. Bhargava, "Analysis of M-ary phase-shift keying with diversity reception for land-mobile satellite channels," *IEEE Trans. Veh. Technol.*, vol. 46, pp. 910–922, Nov. 1997.

[73] D. Aszetly, *On antenna arrays in mobile communication systems: fast fading and GSM base station receiver algorithm*, Ph.D. thesis, Royal Institute Technology, Stockholm, Sweden, Mar. 1996.

[74] H. Bolcskei and A. Paulraj, "Performance of space-time codes in the presence of spatial fading correlation," in *Asiloman Conference on Signals, Syst., Compt.*, Pacific Grove, CA, USA, 2000, vol. 1, pp. 687 – 693.